JOURNAL OF GEOPHYSICAL RESEARCH, VOL. 95, NO. B2, PAGES 1271-1300, FEBRUARY 10, 1990

Evolution of Mauna Kea Volcano, Hawaii: Petrologic and Geochemical Constraints on Postshield Volcanism

F. A. FREY,[1] W. S. WISE,[2] M. O. GARCIA,[3] H. WEST,[3] S.-T. KWON,[2] AND A. KENNEDY,[1]

All subaerial lavas at Mauna Kea Volcano, Hawaii, belong to the postshield stage of volcano construction. This stage formed as the magma supply rate from the mantle decreased. It can be divided into two substages: basaltic (~240-70 ka) and hawaiitic (~66-4 ka). The basaltic substage (Hamakua Volcanics) contains a diverse array of lava types including picrites, ankaramites, alkalic and tholeiitic basalt, and high Fe-Ti basalt. In contrast, the hawaiitic substage (Laupahoehoe Volcanics) contains only evolved alkalic lavas, hawaiite, and mugearite; basalts are absent. Sr and Nd isotopic ratios for lavas from the two substages are similar, but there is a distinct compositional gap between the substages. Lavas of the hawaiitic substage can not be related to the older basalts by shallow pressure fractionation, but they may be related to these basalts by fractionation at moderate pressures of a clinopyroxene-dominated assemblage. We conclude that the petrogenetic processes forming the postshield lavas at Mauna Kea and other Hawaiian volcanoes reflect movement of the volcano away from the hotspot. Specifically, we postulate the following sequence of events for postshield volcanism at Mauna Kea: (1) As the magma supply rate from the mantle decreased, major changes in volcanic plumbing occurred. The shallow magma chamber present during shield construction cooled and crystallized, and the fractures enabling magma ascent to the magma chamber closed. (2) Therefore subsequent basaltic magma ascending from the mantle stagnated within the lower crust, or perhaps at the crust-mantle boundary. Eruptions of basaltic magma ceased. (3) Continued volcanism was inhibited until basaltic magma in the lower crust cooled sufficiently to create relatively low-density, residual hawaiitic melts. Minor assimilation of MORB-related wall rocks, reflected by a trend toward lower $^{206}Pb/^{204}Pb$ in evolved postshield lavas, may have occurred at this time. A compositional gap developed because magma ascent was not possible until a low-density hawaiitic melt could escape from a largely crystalline mush. Eruption of this melt created aphyric hawaiite and mugearite lavas which incorporated cumulate gabbro, wherlite, and dunite xenoliths during ascent.

1. INTRODUCTION

The Hawaiian Ridge is the type example of a hot spot trace [*Wilson*, 1963; *Christofferson*, 1968; *Morgan*, 1972]. Geochemical studies of lavas erupted along this trace provide important information on the mantle sources of hot spot volcanism [e.g., *Tatsumoto*, 1978; *Feigenson*,1986; *Stille et al.*, 1986; *Frey and Roden*, 1987]. In order to evaluate geochemical differences between Hawaiian volcanoes, it is necessary to understand how individual Hawaiian volcanoes evolve and the processes controlling their evolution. The growth stages of a Hawaiian volcano are well defined [*Macdonald et al.*, 1983, pp. 145-154; *Clague and Dalrymple*, 1987]. The most voluminous is the shield stage (the terminology used here is that of *Clague and Dalrymple* [1987]), which is dominated by tholeiitic basalt and is characterized by a high magma supply rate (Figure 1). Toward the end of this stage, eruption rates diminish, rift zones become less active, and eruptions are more widely distributed. The subsequent postshield stage forms a relatively thin veneer of lavas (<10 m to 1 km), including tholeiitic, transitional, and alkalic basalts; hawaiite; mugearite; and rarely, trachyte. The final stage in the eruptive history of some Hawaiian volcanoes (the rejuvenated or posterosional stage) is the eruption of alkalic basalts after a period of volcanic quiescence of up to 2 m.y. [*Clague and Dalrymple*, 1987].

The transition between the shield stage and the postshield stage varies from volcano to volcano. Recent geochemical studies of postshield lavas using stratigraphic sections from Haleakala [*Chen and Frey*, 1983, 1985; *Chen et al.*, 1985; *West and Leeman*, 1987a,b; *Kurz et al.*, 1987] and Kohala volcanoes [*Feigenson et al.*, 1983; *Hofmann et al.*, 1987; *Lanphere and Frey*, 1987; *Spengler and Garcia*, 1988] have shown that the shield and postshield lavas are derived from distinct parental magmas formed by mixing of components from compositionally different mantle sources.

At Mauna Kea the postshield stage can be divided into two substages: the oldest and most voluminous consists largely of basaltic lavas (basaltic substage) and the younger consists

[1]*Department of Earth, Atmospheric, and Planetary Sciences, Massachusetts Institute of Technology, Cambridge.*

[2]*Department of Geological Sciences, University of California, Santa Barbara.*

[3]*Hawaii Institute of Geophysics, University of Hawaii Honolulu.*

Paper number 89JB-1326.
0148-0227/90/89JB-01326$05.00

only of hawaiite and mugearite (hawaiitic substage, Figure 1). Within the basaltic substage the oldest subaerial lavas are intercalated tholeiitic and alkalic basalt. This substage is characterized by a large decrease in eruption rates. Based on data for the currently active shields, Kilauea and Mauna Loa, eruption rates during shield formation are about 30 x 10^6 m^3/yr with magma production rates of about 100 x 10^6 m^3/yr [*Dzurisin et al.*, 1984; *Lockwood and Lipman*, 1987]. In contrast, during the basaltic substage of postshield volcanism at Mauna Kea, about 850 km^3 of lava erupted over ~170 x 10^3 years with eruption rates decreasing from 10 to 2 x 10^6 m^3/yr (Figure 1). A similarly low eruption rate, 2 x 10^6 m^3/yr, has been estimated for recent eruptions at Hualalai volcano [*Moore et al.*, 1987], which appears to be in the basaltic substage of postshield growth. During the hawaiite substage at Mauna Kea, eruption rates have continued to decrease, averaging only ~0.4 x 10^6 m^3/yr (Figure 1 and *West et al.* [1988]).

Previous petrologic and geochemical studies of Mauna Kea were reconnaissance in nature [*Macdonald and Katsura*, 1964; *Macdonald*, 1968; *Budahn and Schmitt*, 1985] or focussed on only one substage (e.g., the hawaiite substage [*West et al.*, 1988]) or one geochemical parameter (e.g., Pb isotopes [*Tatsumoto*, 1978]). Our objective is to use relative age, eruption rates and geochemical data for 149 Mauna Kea lavas to understand the origin and evolution of the postshield stage at Mauna Kea volcano. In other papers we discuss and interpret compositional variations within the hawaiite substage [*West et al.*, 1988] and basalt substage (F.A. Frey et al., manuscript in preparation, 1989). This paper focuses on the transition between the basaltic and hawaiitic substages. Mauna Kea volcano, the highest of the Hawaiian volcanoes and the youngest volcano with a fully developed postshield stage, is ideal for studying this transition. Postshield lavas are well exposed on the dry west side of the volcano and excellent cross sections of these lavas are available in gulches on the wet east flank. We conclude that the marked decrease in eruption rate (Figure 1), presumed to reflect drift of the volanco from the hot spot, caused shallow magma chambers to solidify; subsequent ascending alkalic basalt magmas stagnated at depth, perhaps at the crust-mantle boundary (15-20 km). Crystallization and segregation of dense crystalline phases in these deeper magma chambers formed a low-density hawaiite magma with sufficient buoyancy to erupt and form the hawaiite substage.

2. STRATIGRAPHY AND AGE CONTROL

Stearns and Macdonald [1946] divided the volcanic rocks of Mauna Kea into two units, the Hamakua and Laupahoehoe Volcanic Series. These have been renamed Hamakua Volcanics and Laupahoehoe Volcanics [*Langenheim and Clague*, 1987]. Although in the type section an erosional unconformity separates the two units, *Stearns and Macdonald* [1946] found no widespread uncomformity between the units. Nevertheless, lavas from the two groups are distinctive.

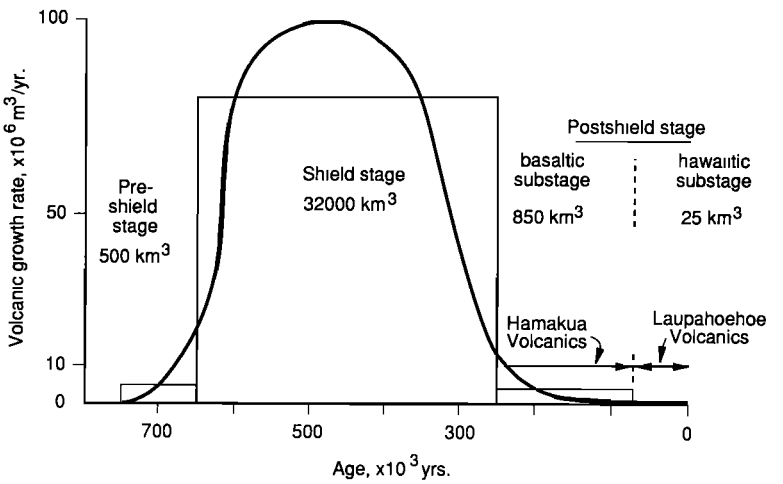

Fig. 1. Growth rate as a function of age for Mauna Kea volcano, illustrating the development of the three volcanic stages (modified from *Wise* [1982]). Rectangles bounded by light lines are proportional to estimated rock volumes for each stage. Heavy line shows variation in supply rate with time. The diagram was constructed by estimating the volume of magma (reduced to dense rock equivalent) added to the edifice during each stage. The preshield stage is assumed to have a volume similar to Loihi. The shield volume was estimated from its present shape adjusted for overlap with neighboring volcanoes and subsidence [*Moore*, 1987]. The estimated time span for the development of the shield stage assumes a maximum magma supply rate equal to the present rate for Kilauea volcano (about 100 x 10^6 m^3/yr [*Swanson*,1972]). In order to allow for a gradual increase at the beginning of the shield stage and a decrease toward the end, the duration is estimated to be ~400,000 years. The end of the shield stage is assumed to have occurred when lava flows were no longer produced at a rate sufficient to maintain the sharp break in slope at sea level, i.e., when subsidence rates exceeded growth rates (*Moore and Fiske*, [1969], and Figure 3). For the preshield and shield stages the volcano growth rate equals the magma supply rate. However, the volume of the postshield stage is based only on extruded lavas; at this stage a significant fraction of the magma supply solidified to form deep crustal cumulates. Details of the postshield stage are based on recent mapping and K-Ar dating (see text).

Lavas of the Lauphahoehoe Volcanics consist only of hawaiite and mugearite; basalt is absent. In contrast, the Hamakua Volcanics are dominantly basalt. All Laupahoehoe flows are virtually aphyric, and they are easily distinguished from phenocryst-bearing Hamakua basalts. Figure 2 shows the outcrop distribution of these two units and their estimated volumes are indicated in Figures 1 and 3.

The Hamakua Volcanics include all the subaerial lavas erupted during the basaltic substage of the postshield volcanism. New K-Ar ages range between about 80 and 240

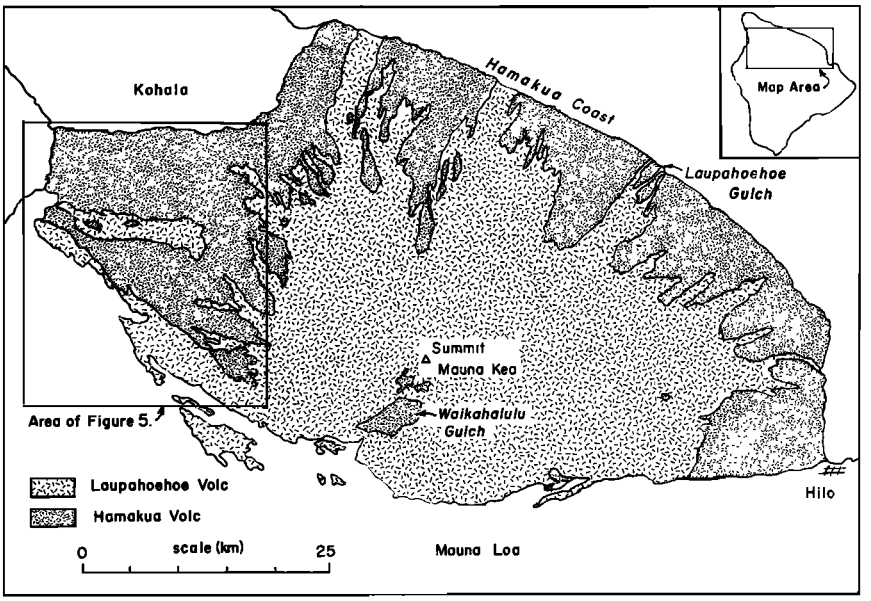

Fig. 2. Map of Mauna Kea volcano, showing the subaerial distribution of lavas of the Hamakua and Laupahoehoe Volcanics, and the location of Waikahalulu Gulch. Lava distributions based on new mapping by E.W. Wolfe and W.S. Wise.

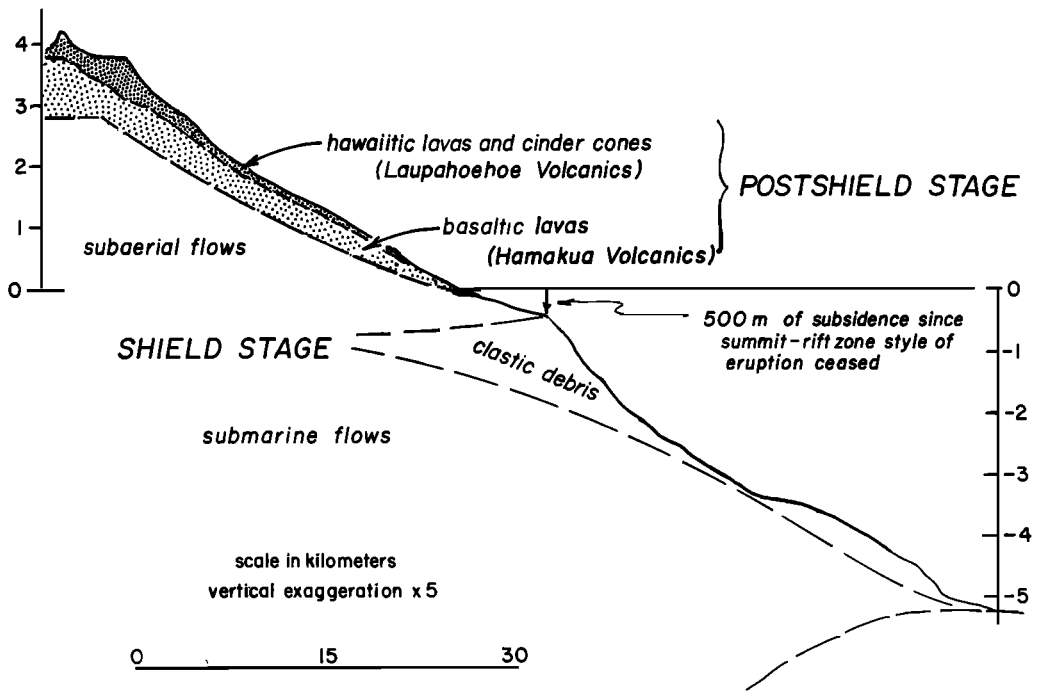

Fig. 3. Cross section through the northeast flank of Mauna Kea, illustrating the relationships between the shield and postshield lavas based on work by *Moore and Fiske* [1969, Figure 3]. The break in slope, presently at a depth of 500 m is assumed to represent sea level when the shield stage was active. A subsidence rate of 2.5 mm/yr for this part of the volcano [*Moore*, 1987] suggests that voluminous flows ceased reaching sea level about 200 ka, a time that must represent the early part of postshield activity. The early postshield flows, exposed in sea cliffs, are basalt, and later flows are exclusively hawaiite and mugearite. These petrologic types comprise the two substages, illustrated in Figure 1, and the formations mapped on the surface (Figures 2 and 5).

ka (E.W. Wolfe et al., The geology and petrology of Mauna Kea volcano, Hawaii: A study of postshield volcanism, submitted to *U.S. Geological Survey Professional Paper*, 1989). The oldest reliable age is for an alkalic basalt from a gulch on the Hamakua coast (Figure 2). The best control on the age of the uppermost Hamakua lavas is in Waikahalulu Gulch on the southern flank of the volcano (Figure 2), where recent mapping and interpretation of glacial deposits place a 70 ka age on the uppermost Hamakua flow (Figure 4). Laupahoehoe lavas, comprising the hawaiitic substage of the postshield stage, overlie the Hamakua lavas and range in age from about 66 (±8) ka (sample NO-10, Table 1 (E.W. Wolfe et al., submitted manuscript, 1989)) to 4 ka [*Porter*, 1979]. Therefore the time interval between the eruption of the last Hamakua lava and the earliest Laupahoehoe lava is likely to have been less than 5000 years.

3. SAMPLING

The northwest flank of Mauna Kea is well exposed and enables evaluation of the temporal variation in composition across the transition from Hamakua alkalic basalts to Laupahoehoe hawaiites and mugearites. Phenocryst abundances within a single flow are sufficiently consistent to permit mapping of flows, even in areas of limited outcrops. Similarly, the variation of phenocryst abundances between flows, coupled with surface characteristics, allows the tracing of flow boundaries over long distances (up to 20 km). At least 75 Hamakua flows and seven Laupahoehoe flows are exposed in this area (Figure 5). The stratigraphic relationships of 36 flows are subdivided into three sequences: (1) along Kamakoa Gulch (samples 1-13), (2) Hapuna Bay to Waimea (samples 14-26), and (3) in the vicinity of Waikii (samples 27-36) (see Figures 5 and 6). Ages of these basaltic substage lavas range from 150 to 81 ka (Wolfe et al., submitted manuscript, 1989).

Stream erosion enhanced by melting glaciers which capped the volcano down to the 3400-m level [*Porter*, 1979] cut the 75-m-deep Waikahalulu Gulch into the south slope of Mauna Kea between the elevations of 3100 and 2750 m (Figure 2). The walls of the gulch expose an 85-m section of Hamakua Volcanics intercalated with two glacial members, overlain by two Laupahoehoe hawaiite flows (Figure 4). A stratigraphically controlled suite of lavas was collected from Waikahalulu Gulch in order to evaluate the transition in lava composition from Hamakua basalt to Laupahoehoe hawaiite. *Porter* [1979] had previously delineated the boundary between Hamakua Volcanics and Laupahoehoe Volcanics at the top of the Pohakaloa glacial deposit (Figure 4). There is a macroscopic change in the character of the lavas from mostly porphyritic to weakly porphyritic or aphyric above this boundary. Other Hamakua lavas collected from the south flank are a strongly olivine-phyric sample, H-1, from the lower slope, aphyric samples, H-2 and H-3, from the middle slopes, and an olivine-phyric sample, 65-1, from the upper slope.

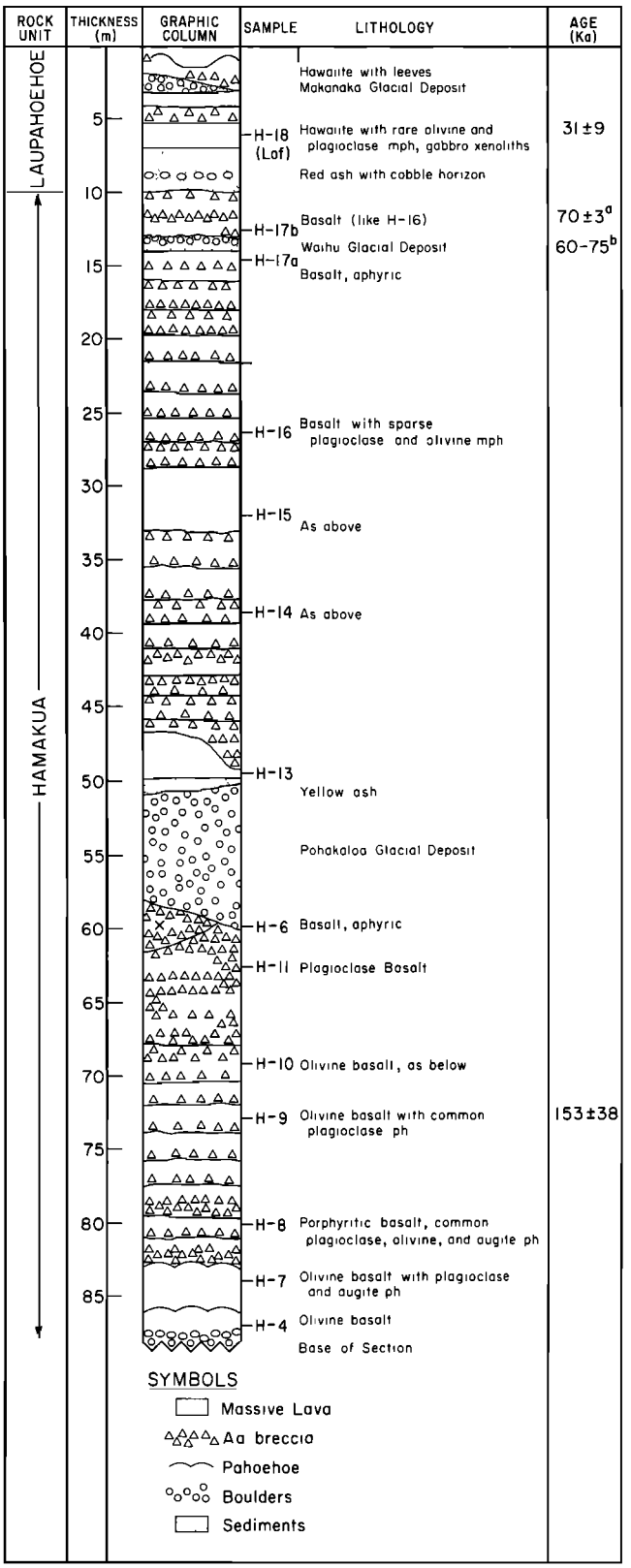

Fig. 4. Stratigraphic section in Waikahalulu Gulch, upper south flank of Mauna Kea volcano (see Figure 2). Section shows the transition zone between Hamakua and Laupahoehoe lavas which is marked by a red ash horizon. Three glacial deposits provided good stratigraphic markers on the upper slopes of the volcano. The age of the Waihu deposit (b) probably correlates with an oxygen isotope stage 6 (60-75 ka [Martinson et al., 1987]. The other ages are K-Ar dates on lavas (a, *Porter*, [1979]; others, E.W. Wolfe et al., submitted manuscript, 1989)). Sample location for H-6 is marked by a cross. Analyses for numbered samples are in Table 1*b*.

TABLE 1a. Major Oxide (wt.%) and Trace Element (ppm) Contents of Hamakua Lavas (Basaltic Substage) From the West Flank of Mauna Kea Volcano

	Waikoloa Section Samples												
	1	2	3	4	5	6	7	8	9	10	11	12	13
Field	115-4	115-3	115-20	97-2	115-6	115-23	115-25	71-9	NO-14	NO-13	83-17	73-2	73-4
SiO_2	47.23	47.79	47.01	47.48	45.73	47.60	47.84	47.47	46.97	45.54	46.10	46.6	45.39
TiO_2	2.31	3.54	3.30	2.98	4.57	3.28	3.62	3.46	3.71	3.24	4.56	3.78	3.26
Al_2O_3	12.64	14.07	13.73	14.14	14.61	14.21	13.77	13.98	14.44	14.44	14.86	14.2	14.38
Fe_2O_3	12.20	14.60	13.67	12.82	15.83	13.30	14.81	13.91	13.86	13.81	15.69	14.1	13.71
MnO	0.16	0.20	0.18	0.18	0.22	0.19	0.20	0.19	0.19	0.19	0.22	0.18	0.19
MgO	11.23	5.17	7.26	7.46	5.05	6.05	5.57	5.81	5.74	8.16	5.15	5.72	8.04
CaO	11.63	10.24	11.16	11.56	8.28	11.15	10.37	10.72	10.73	10.90	8.31	11.0	10.93
Na_2O^a	1.68	2.83	2.43	2.23	3.32	2.51	2.52	2.47	2.93	2.59	3.13	2.90	2.54
Na_2O^b	2.00				3.47		2.80		2.98	2.58	3.26		
K_2O	0.50	1.00	0.82	0.75	1.41	0.81	0.96	0.87	0.98	0.90	1.42	0.97	0.85
P_2O_5	0.27	0.49	0.42	0.38	0.75	0.42	0.47	0.46	0.49	0.42	0.75	0.52	0.42
Sum	99.86	99.94	99.99	99.97	99.77	99.50	100.12	99.32	100.20	100.19	100.19	99.97	99.76
H_2O^+	0.13	0.31	0.17	0.31	0.10	0.07		0.25	0.19	0.13	0.34		0.20
Rb	9.0	18.5	14.5	11.5	25.3	14.8	18.5	15.9	14.9	16.8	25.9		13.5
Sr	455	591	592	547	696	570	590	566	635	628	693		619
Ba	174	327	288	247	485	271	309	276	323	293	476		287
Sc	32.3				21.3		27.2		27.6	28.9±.01	21.2		
V	252	295	298	292	234	310	346	317	320	285	232		294
Cr	761	40	141	225	3	77	59	50	92	366±8	<1		318
Co	60.6				45.6		48.9		45.0	55.4±0.4	44.3		
Ni	296	49	113	136	43	81	53	71	72	147	45		140
Zn	97	128	104	121	138	109	129	121	121	120	154		114
Ga	18.8	25.7	22.9	22.0	28.2	22.9	23.5	23.8	23.7	22.9	26.5		22.5
Y	20	33	28	26	40	28	31	30	32	28	40		28
Zr	152	282	239	229	395	239	271	260	295	255	392		251
Nb	17.1	34.2	27.1	25.9	50.5	26.9	31.1	28.7	33.7	29.3	49.8		29.9
Hf	3.7				9.0		6.3		6.5	5.62±.06	8.8		
Ta	0.87				2.9		1.65		1.94	1.63±.10	3.0		
Th	0.4				3.6		1.6		1.9	1.4±0.2	3.4		
La	14.0				41.6		26.2		28.4	24.5±0.1	40.5		
Ce	36.6	73	58	59	106	60	67	63	71.8	61.0±0.2	104		62
Nd	21.3				57		37.1		40.3	34.3±0.9	57		
Sm	5.24				12.2		8.73		9.02	7.94±.03	12.4		
Eu	1.87				3.93		2.88		2.97	2.63±.02	3.94		
Tb	0.82				1.58		1.27		1.32	1.06±.01	1.47		
Ho	0.7				1.3		1.2		1.34	1.1±0.1	1.5		
Yb	1.61				3.04		2.31		2.43	2.13±.09	3.01		
Lu	0.20				0.41		0.33		0.31	0.278±.005	0.41		

Except for samples 36 [*Macdonald*, 1968] and 12 (USGS unpublished) in Table 1a all data in Tables 1a, 1b, and 1c were obtained by duplicate XRF analyses at University of Massachusetts, except for Sc, Co, Hf, Ta, Th, La, Nd, Sm, Eu, Tb, Ho, Yb, and Lu, which were determined by INAA at MIT. Na_2O data obtained by XRF[a] and INAA[b] are reported; also, when available, tabulated Cr and Ce data are INAA determinations. Mean and one standard deviation of duplicate INAA data for NO-13 are indicated. For a more general evaluation of accuracy and precision, see Table 1d. All Hamakua lavas are basaltic. Samples 5, 11, and 16 are the high Fe-Ti basalts discussed in the text, and samples 20, 21, and 36 are ankaramites. Sample locations are indicated in Figure 5.

[a]Data by XRF

[b]Data by neutron activation

4. RESULTS

4.1. Petrography and Mineral Compositions

Petrographic examination and chemical analyses reveal three broad lava types within the Hamakua Volcanics on the northwest slope (Table 1 and Figure 6). In order of relative abundance they are (1) weakly to moderately porphyritic basalts; typically containing 2-10% olivine, augite, and plagioclase phenocrysts or microphenocrysts; (2) strongly to extremely porphyritic ankaramites; and (3) high Fe-Ti basalts which are nearly aphyric and dark grey to black and form small volume flows (Figure 5). They typically have 4.5-5% TiO_2 and over 15% total iron (as Fe_2O_3) and a normative plagioclase composition less than An_{50}, typically near An_{45}.

New representative mineral compositions for Hamakua

TABLE 1a. (continued)

	Hapuna to Waimea Section Samples												
	14	15	16	17	18	19	20	21	22	23	24	25	26
Field	115-35	115-36	115-14	115-11	115-37	KW-1	115-12	97-14	114-9	114-2	85-10	85-2	83-27
SiO_2	48.26	47.96	45.24	47.50	47.60	47.06	46.77	46.30	47.82	47.05	47.10	47.51	47.11
TiO_2	2.81	2.77	4.71	3.38	3.43	3.12	1.90	1.86	2.40	3.17	2.32	3.27	3.27
Al_2O_3	14.32	14.27	14.32	15.42	13.52	13.54	10.57	10.23	12.60	13.08	10.12	13.75	13.76
Fe_2O_3	12.34	12.56	16.56	13.67	14.44	13.25	12.02	12.09	13.15	12.72	12.72	13.17	13.33
MnO	0.17	0.18	0.23	0.19	0.20	0.19	0.16	0.16	0.16	0.17	0.18	0.18	0.18
MgO	6.80	7.20	5.09	5.25	6.31	7.68	15.25	15.88	10.66	8.77	14.35	7.70	7.79
CaO	11.81	11.76	8.13	11.02	10.55	11.34	10.88	10.95	11.72	10.90	10.83	10.95	10.92
Na_2O^a	2.25	2.13	3.34	2.74	2.48	2.46	1.76	1.36	1.71	2.12	1.63	2.38	2.53
Na_2O^b			3.42				1.66	1.60					2.75
K_2O	0.71	0.67	1.43	0.83	0.89	0.84	0.46	0.42	0.54	0.77	0.57	0.81	0.83
P_2O_5	0.35	0.32	0.74	0.40	0.44	0.43	0.22	0.23	0.30	0.40	0.30	0.45	0.44
Sum	99.83	99.82	99.79	100.31	99.87	99.91	99.98	99.48	99.99	99.58	100.12	100.19	100.16
H_2O^+		0.11	0.15	0.17	0.38	0.09	0.16	0.22	0.23	0.36	0.07	0.15	0.13
Rb	13.8	11.9	28.8	14.3	17.2	15.3	8.6	6.6	9.6	14.7	11.4	14.1	12.3
Sr	552	537	687	654	578	582	384	380	468	542	404	569	570
Ba	244	217	487	254	291	300	173	171	180	254	213	275	290
Sc			21.1				31.4	32.3					29.0
V	277	284	274	331	327	292	222	221	247	278	247	293	302
Cr	92	294	22	56	124	348	1167	1220	642	389	1384	246	331
Co			49.5				70.8	72.5					50.4
Ni	99	116	56	51	80	139	486	501	274	202	408	143	165
Zn	101	102	142	109	123	105	103	99	95	113	98	112	111
Ga	22.2	20.7	26.6	24.7	21.7	21.6	15.6	16.9	19.1	22.8	16.7	23.2	22.2
Y	25	25	41	28	30	28	17	16	22	28	20	28	28
Zr	201	197	395	218	259	242	135	131	171	246	168	241	254
Nb	24.2	20.8	49.2	24.8	30.8	30.1	17.0	16.6	18.6	26.7	21.3	26.8	30.5
Hf			9.0				3.1	3.1					6.0
Ta			3.0				0.98	0.85					1.72
Th			2.7				0.6	0.5					1.2
La			40.8				13.7	13.5					26.3
Ce	54	47	102	55	64	66	35	33.2	42	61	44	55	65
Nd			55				19.9	18.6					34.5
Sm			12.2				4.58	4.47					8.17
Eu			3.88				1.58	1.56					2.75
Tb			1.73				0.61	0.66					1.10
Ho			1.4				0.5	0.7					1.1
Yb			3.11				1.27	1.27					2.26
Lu			0.44				0.19	0.19					0.31

lavas are given in Table 2. In general, plagioclase phenocrysts in Hamakua basalts are bytownites (An_{83-75}) with groundmass crystals in the middle labradorite range; however, the high Fe-Ti basalts contain labradorite phenocrysts (An_{67-61}). Olivine phenocryst compositions in basalts are typically Fo_{87-84}, and they do not vary with olivine abundance. Groundmass crystals range between Fo_{80} and Fo_{75}. In the high Fe-Ti basalts, rare phenocrysts are Fo_{76} to Fo_{72}, and groundmass crystals are Fo_{72} to Fo_{65}. Augite analyses show little variation between flows and are typical of clinopyroxenes from mildly alkaline basalts; phenocryst cores average $Wo_{42}En_{51}Fs_7$, while rims and groundmass compositions are only slightly more iron-rich. Titanomagnetite and ilmenite occur as groundmass phases in most of the lavas; in addition, microphenocrysts of titanomagnetite and inclusions of ilmenite in clinopyroxene occur in the high Fe-Ti basalts. In several lavas, coexisting ilmenite and titanomagnetite in the groundmass appear to be in textural and compositional equilibrium [*Bacon and Hirschmann*, 1988]. Temperature and oxygen fugacity estimates are 997°C and log f_{O_2}= -11.2 for sample C, a Laupahoehoe hawaiite, and 1065°C and log f_{O_2} = -10.0 to -10.3 for samples 5 and 26, a high Fe-Ti Hamakua basalt and Hamakua basalt, respectively, (calculations used the GPP program of D.J. Geist et al., 1985). Thus these Mauna Kea lavas evolved close to the QFM buffer.

Laupahoehoe lavas are nearly aphyric; most contain less than 1% phenocrysts. Plagioclase (An_{59} to An_{57}) is dominant with minor olivine (Fo_{81} to Fo_{75}) and Ti-rich (17-19% TiO_2) magnetite [*West et al.*, 1988].

TABLE 1a. (continued)

	Waikii Section Samples									
	27	28	29	30	31	32	33	34	35	36
Field	81-36	81-46	81-19	KM-5	81-30	KM-9	NO-9	NO-11	NO-5	C-207
SiO_2	45.99	45.36	47.48	47.30	47.45	47.75	50.01	47.34	47.25	46.18
TiO_2	3.23	3.46	3.24	3.10	3.70	3.63	3.11	2.96	3.32	3.98
Al_2O_3	13.65	14.81	14.21	14.25	14.24	13.64	14.29	15.74	13.88	13.90
Fe_2O_3	14.14	14.11	14.15	13.84	13.61	14.95	13.52	13.09	13.48	15.14
MnO	0.20	0.18	0.20	0.18	0.18	0.20	0.21	0.17	0.19	0.18
MgO	8.32	7.45	6.42	6.56	5.71	5.31	4.26	5.63	6.91	5.57
CaO	10.84	10.55	10.99	11.16	10.80	10.00	8.78	11.69	11.35	10.49
Na_2O^a	2.48	2.49	2.41	2.27	2.61	2.72	3.29	2.42	2.57	3.00
Na_2O^b						2.85	3.56	2.55	2.56	
K_2O	0.82	0.94	0.79	0.75	0.98	0.95	1.35	0.72	0.82	1.02
P_2O_5	0.42	0.46	0.40	0.38	0.50	0.46	0.75	0.36	0.40	0.56
Sum	100.1	99.82	100.28	99.79	99.78	99.61	99.57	100.12	100.30	100.02
H_2O^+	0.16	0.19	0.21	0.19	0.20	0.22	0.29	0.13	0.07	0.63
Rb	13.1	17.1	13.4	14.0	17.7	17.9	26.0	12.7	14.3	
Sr	549	657	581	581	615	574	604	623	601	
Ba	267	326	261	240	326	303	425	263	302	
Sc						27.9	23.0	28.4	29.4	
V	307	292	321	291	308	336	239	274	263	
Cr	277	207	135	180	66	54.8	19	139	195	
Co						49.4	37.0	45.6	48.3	
Ni	149	131	88	99	72	58	31	65	102	
Zn	123	127	116	111	112	134	143	96	106	
Ga	22.4	23.2	22.5	22.4	24.5	23.6	25.5	25.1	23.6	
Y	29	30	28	28	33	33	45	26	29	
Zr	235	275	230	221	291	278	386	198	242	
Nb	26.4	31.9	26.7	24.7	33.2	30.4	43.2	24.8	27.6	
Hf						6.3	9.0	4.7	5.5	
Ta						1.77	2.5	1.42	1.60	
Th						1.7	3.5	1.5	1.5	
La						26.5	40.9	20.9	23.1	
Ce	57	63	54	56	73	65.6	101	53.3	59.9	
Nd						37.8	55.7	30.5	34.5	
Sm						8.54	12.5	7.00	7.92	
Eu						2.91	4.04	2.34	2.54	
Tb						1.26	1.60	0.94	1.03	
Ho						1.3	2.0	0.96	1.07	
Yb						2.47	3.62	1.93	2.13	
Lu						0.35	0.47	0.26	0.31	

4.2. Lava Compositions: Analytical

Samples (149) were analyzed by X ray fluorescence at the University of Massachusetts [*Rhodes*, 1983] for major elements and the trace elements Rb, Sr, Ba, V, Ni, Zn, Ga, Y, Zr, and Nb (Tables 1*a*-1*c*). All samples were analyzed in duplicate and typical precisions are indicated in Table 1*d*. A subset of lavas (98) were analyzed for Sc, Cr, Co, Hf, Ta, Th, and rare earth elements (REE) by instrumental neutron activation analysis at the Massachusetts Institute of Technology [*Ila and Frey*, 1984]; see Table 1*d* for precision estimates. The mean of multiple analyses of a Hawaiian tholeiite, *U.S.Geological Survey* standard BHVO-1, is also listed in Table 1d. Isotopic data (Sr, Nd, and Pb) for a subset (38) of these samples are discussed by A.K. Kennedy et al. (manuscript in preparation, 1989).

4.3. Lava Compositions: Results

In this section we discuss major and trace element abundance trends for Mauna Kea samples from the northern and western flanks (Tables 1*a* and 1*c*), Waikahalulu Gulch (Table 1*b*), samples of the Laupahoehoe Volcanics from the summit and south rift [*West et al.*, 1988] and samples of the Hamakua Volcanics from gulches on the deeply eroded northeast coast (F.A. Frey et al., manuscript in preparation, 1989).

Major elements and compatible trace elements. Lavas of the Hamakua Volcanics straddle the tholeiitic-alkalic dividing line (Figure 7). Some samples in the tholeiitic field are clinopyroxene-rich and contain more than 10% MgO (e.g., samples 114-9, 115-4, and 97-14 in Table 1*a*); they may plot in the tholeiitic field because of clinopyroxene accumulation.

TABLE 1b. MAJOR OXIDE (wt.%) AND TRACE ELEMENT (ppm) CONTENTS OF LAVAS FROM

	Samples										
	Hamakua[a]									Hamakua[b]	
	H-1	65-1	H-2	H-3	H-4	H-7	H-8	H-9	H-10	H-11	H-6
SiO_2	43.79	46.38	48.07	47.82	48.08	48.72	48.63	48.80	48.53	48.01	47.35
TiO_2	2.41	1.86	3.21	3.02	2.56	2.81	2.66	2.53	2.74	3.12	3.58
Al_2O_3	9.57	8.94	14.46	13.39	11.96	13.99	12.50	13.27	12.77	14.23	14.10
Fe_2O_3	13.77	13.34	13.48	13.65	13.06	12.47	12.66	12.06	12.72	13.94	13.79
MnO	0.19	0.18	0.18	0.18	0.18	0.19	0.18	0.17	0.19	0.19	0.19
MgO	17.84	17.93	5.99	6.59	9.98	7.07	8.31	7.90	7.96	5.66	6.15
CaO	9.91	9.65	11.25	11.73	11.51	11.79	12.27	12.51	12.24	11.18	11.04
Na_2O[c]	1.20	1.43	2.32	2.05	1.75	2.18	1.82	2.00	1.98	2.21	3.14
Na_2O[d]	1.45		2.52	2.33	1.92	2.33	2.02	2.20	2.10	2.46	2.88
K_2O	0.47	0.35	0.78	0.59	0.56	0.60	0.55	0.51	0.57	0.75	0.96
P_2O_5	0.30	0.23	0.39	0.35	0.31	0.32	0.31	0.28	0.32	0.38	0.50
Sum	99.70	100.28	100.33	99.65	100.12	100.29	100.09	100.23	100.14	99.92	100.54
H_2O^+	0.41	0.17	0.20	0.26	0.30	0.15	0.54	0.36	0.24	0.29	0.17
Rb	5.9	6.0	14.7	10.2	9.6	10.2	10.0	8.3	9.4	13.2	16.7
Sr	440	296	556	454	398	462	412	431	426	496	646
Ba	265	154	265	191	173	201	168	162	172	235	315
Sc	27.7		28.0	32.7	33.5	31.3	36.2	34.3	30.1	26.5	29.4
V	256	222	299	294	270	282	291	285	301	294	294
Cr	1140	1220	89	168	667	358	471	416	386	68	67
Ni	660	551	77	86	222	121	141	123	128	73	80
Zn	116	106	114	127	112	119	114	103	110	124	118
Ga	16.3	17.6	23.2	21.5	20.1	21.9	20.0	20.7	20.6	22.0	24.2
Y	16.4	19	29.3	28.2	24.6	25.6	25.0	22.9	25.5	29.1	29.2
Zr	179	130	240	215	182	192	185	171	187	229	276
Nb	26.3	13.1	27.1	21.8	18.2	20.7	19.8	17.5	19.5	25.0	30.9
Hf	3.9		5.4	5.0	4.1	4.6	4.3	3.96±0.06	4.1	5.4	6.2
Ta	1.7		1.9	1.5	1.4	2.1	2.5	2.01±.01	2.1	2.6	2.1
Th	1.2		1.6	1.1	0.9	0.8	0.9	0.7	1.0	1.4	2.1
La	19.6		23.3	18.4	15.4	16.4	15.9	14.55±.03	15.4	20.7	25.7
Ce	45.0	36	56.5	46.3	38.7	41.5	40.1	36±1	39.6	52.1	67.6
Nd	24.9		32.8	28.2	23.6	24.7	23.9	22.1±.3	24.5	30.5	36.6
Sm	5.32		7.57	6.77	5.83	6.28	6.03	5.7±.2	6.17	7.48	8.45
Eu	1.83		2.63	2.47	2.05	2.22	2.16	2.10±.03	2.13	2.57	2.80
Tb	0.72		1.0	0.98	0.93	1.06	1.05	0.9±.01	0.88	1.07	1.05
Ho	0.6		1.0	1.1	1.0	1.0	1.3	0.96±.03	1.1	1.1	1.1
Yb	1.23		2.16	2.18	1.77	1.91	1.89	1.74±.01	1.91	2.19	2.04
Lu	0.16		0.29	0.30	0.26	0.26	0.26	0.25±.02	0.26	0.32	0.28

Samples H-1 and 65-1 are picrites; all other Hamakua lavas are basaltic; the two Laupahoehoe lavas are hawaiites.
[a]Stratigraphic position relative to other samples is uncertain.
[b]Samples arranged in stratigraphic order (see Figure 4).
[c]Data by XRF
[d]Data by neutron activation

However, some lavas of the Hamakua Volcanics from deep exposures on the east coast (F.A. Frey et al., manuscript in preparation, 1989) and younger lavas from Waikahalulu Gulch (samples H-4,7,8,9, and 10 in Table 1*b*) plot in the tholeiitic field and do not contain abundant clinopyroxene. Six samples of the Hamakua Volcanics have high Na_2O+K_2O and relatively low SiO_2 (e.g., samples 83-17, 115-6, and 115-14, Table 1*a*). They form a distinctive group of high Fe-Ti basalts which are compositionally distinct from other Hamakua lavas and the overlying lavas of the Laupahoehoe Volcanics (Figure 7).

Many of the lavas in Waikahalulu Gulch that were mapped as Laupahoehoe lavas by *Porter* [1979] are actually Hamakua basalts. Specifically, samples H-13 to H-17b from above the Pohakaloa glacial deposit (Figure 4) fall within the Hamakua fields on Figures 7-9. Only the uppermost analyzed sample, H-18, is a Laupahoehoe hawaiite. Therefore the duration, areal extent, and volume of the Laupahoehoe Volcanics are considerably smaller than previously proposed. Unfortunately, this "contact" between the Hamakua and Laupahoehoe volcanics is not always distinct in the field when aphyric Laupahoehoe hawaiites and mugearites overlie aphyric Hamakua basalt. Nevertheless, there is a distinct compositional break at this contact (Table 1*b*, Figures 7-13). Because of our good stratigraphic control, especially at Waikahalulu Gulch (Figure 4), we are confident that the compositional gap between Hamakua and Laupahoehoe lavas is not a result of inadequate sampling.

Lavas of the Laupahoehoe Volcanics define a distinct field with high alkali content and relatively high SiO_2 (Figure 7). Following the classification of *LeBas et al.* [1986] they are hawaiites and mugearites. The mugearite lava, sample NO-10 (Figures 7 and 8), defines the most evolved end of the Laupahoehoe field. Based on samples from the summit, west and south rifts there are no temporal or spatial variations in the composition of Laupahoehoe lavas (Table 1*c* and *West et*

WAIKAHALULU GULCH OF MAUNA KEA VOLCANO

										Laupahoehoe[b]	
H-13	65-3	H-14	65-4	H15	H16	H17	Mhf	H17a	H17b	H18	Lof
47.50	47.05	47.21	47.82	47.51	47.13	48.36	47.03	47.35	48.34	49.26	49.55
3.31	3.73	3.67	3.54	3.67	3.49	3.76	3.61	3.79	3.75	2.89	2.84
14.55	14.54	13.95	14.14	14.08	14.05	13.80	13.64	13.99	13.73	17.06	17.10
13.79	13.63	15.06	14.08	14.37	14.49	14.77	15.37	15.29	14.78	11.71	11.52
0.19	0.18	0.21	0.20	0.19	0.20	0.21	0.20	021	0.21	0.20	0.20
5.91	6.03	5.64	5.67	5.59	5.83	4.80	5.48	5.52	4.84	4.24	4.20
11.00	10.89	10.51	10.47	10.37	10.82	9.40	10.27	10.23	9.39	7.16	7.04
2.56	2.54	2.55	2.65	3.02	3.21	3.35	2.94	2.86	3.26	4.81	5.07
2.66		2.75		2.80	2.68	2.96	2.76	2.79	3.02	4.45	
0.67	0.67	0.72	0.92	0.87	0.73	1.07	0.86	0.76	1.10	1.82	1.87
0.40	0.34	0.46	0.43	0.43	0.40	0.70	0.45	0.47	0.68	0.86	0.86
99.98	99.60	100.18	99.91	99.89	99.84	99.83	99.69	100.40	99.84	99.65	100.25
0.24			0.19								
6.4	8.6	8.9	15.7	13.0	8.8	16.6	14.1	8.6	18	32.6	32.9
552	624	624	87	577	559	594	571	559	582	1286	1273
260	315	226	329	352	259	354	283	305	353	586	595
29.4		29.3		28.1	29.6	24.7	29.6	28.6	25.2	10.5	
327	343	360	357	350	360	320	369	366	330	101	101
47	115	28	5	46	32	24	31	24	24	12	3
65	75	53	61	71	74	44	65	53	40	16	16
137	116	140	122	126	130	142	137	141	148	117	116
23.1	24.2	23.7	25.0	22.7	23.9	24.6	24.8	24.1	25.0	21.0	20.7
29.9	28	32.4	31	32.2	32.0	39.5	32.4	34.4	37.8	44.0	45.8
246	204	269	245	246	247	339	262	291	343	430	444
26.7	21.6	30.1	31.5	31.5	27.7	38.0	31.1	31.1	38.3	57	56
5.6		6.0		5.8	5.5	7.6	6.2	6.5	7.6	9.3	
3.0		4.0									
1.9		12.9		1.8	1.7	2.3	2.0	2.1	2.6	3.5	
21.8		24.8		24.2	21.8	31.6	24.9	25.6	32.0	45.1	
53	46	62	58	60.8	57.4	81.7	64.0	63.9	77.4	111	
32		36		36.3	36.0	48.7	38.9	38.7	48.1	67	
7.70		8.49		8.27	7.86	10.67	8.55	9.21	10.8	13.9	
2.70		2.93		2.71	2.59	3.34	2.81	3.03	3.39	4.42	
1.07		1.20		1.00	1.07	1.33	1.12	1.27	1.34	1.62	
1.0		1.1									
2.37		2.59		2.41	2.28	2.76	2.30	2.72	2.96	3.11	
0.32		0.35		0.34	0.32	0.44	0.34	0.37	0.44	0.42	

al. [1988]). Only Hamakua lava NO-9 is intermediate in composition between the Hamakua and Laupahoehoe groups (Figure 7).

The following discussion summarizes trends of Mauna Kea lavas in MgO variation diagrams (Figure 8*b*).

SiO_2: The major feature is the coherent trend of increasing SiO_2 with decreasing MgO defined by Laupahoehoe lavas. The large scatter in the Hamakua lavas is in part caused by the six high Fe-Ti basalts which have low SiO_2 at 5-6% MgO. In this plot these samples are not intermediate between the Laupahoehoe lavas and other Hamakua lavas. Much of the scatter among Hamakua lavas reflects the intercalation of tholeiitic and alkalic lavas and accumulative phases in ankaramites (F.A. Frey et al., manuscript in preparation, 1989).

Al_2O_3: There is a well-defined trend of increasing Al_2O_3 with decreasing MgO, and a distinct gap separates Hamakua lavas from the hawaiites of the Laupahoehoe volcanics.

CaO: Hamakua basalts, ankaramites and picrites define a broad trend of increasing CaO with decreasing MgO. The large variation of CaO at a given MgO content (for MgO >5%) is partially caused by accumulative clinopyroxene and olivine (F.A. Frey et al., manuscript in preparation, 1989). In contrast, below 5% MgO there is a precipitous decrease in CaO with decreasing MgO, and the Laupahoehoe hawaiites and mugearites form a distinct group at 5-7.3% CaO. Several Hamakua lavas; specifically the high Fe-Ti basalts and sample NO-9, occupy an intermediate position. As a consequence, Mauna Kea lavas vary widely and systematically in Al_2O_3/CaO (Figure 8*a*). Ratios <1 are found in clinopyroxene-rich lavas (ankaramites) and probably reflect clinopyroxene accumulation (Frey et al., manuscript in preparation, 1989). Ratios from 1.4 to 1.8 characterize Hamakua sample NO-9 and the high Fe-Ti basalts. A major gap separates the Laupahoehoe lavas (Al_2O_3/CaO = 2.3 to 3) from the Hamakua lavas; the most extreme ratio 3.4 occurs in the mugearite NO-10.

TiO_2 and Fe_2O_3 (total iron): With increasing MgO, Hamakua lavas increase in TiO_2, but Fe_2O_3 does not define a coherent trend. In both plots the high Fe-Ti Hamakua basalts form a distinct group at the high Fe_2O_3 and TiO_2 extremes of these trends. In contrast, Laupahoehoe hawaiites and mugearites define well-constrained steep trends of decreasing Fe_2O_3 and TiO_2 with decreasing MgO.

Na_2O and K_2O: In Hamakua lavas Na_2O and K_2O tend to increase with decreasing MgO. However, the K_2O trend is

TABLE 1c. Major Oxide (wt.%) and Trace Element (ppm) Contents of Laupahoehoe Lavas (Hawaiitic Substage) From the West Flank of Mauna Kea Volcano

	Sample							
	A	B	C	D	E	F	G	H
Field	NO-10	NO-4	PH-1	KM-6	81-47	75-2	101-3	81-32
SiO_2	54.17	49.78	49.48	49.96	51.73	49.04	49.70	49.82
TiO_2	1.60	2.71	2.85	2.76	2.26	2.90	2.78	2.76
Al_2O_3	17.11	17.13	16.91	17.07	17.23	16.86	16.94	16.97
Fe_2O_3	9.58	11.82	11.85	11.81	10.36	11.93	11.68	11.72
MnO	0.22	0.21	0.21	0.22	0.23	0.21	0.22	0.22
MgO	2.63	3.76	4.17	3.99	3.15	4.22	3.94	4.04
CaO	5.00	6.86	6.98	6.86	6.39	7.12	6.91	6.88
Na_2O^a	5.48	4.50	4.62	4.72	5.02	4.23	4.49	4.32
NA_2O^b	5.43		4.55	4.47				
K_2O	2.55	1.89	1.81	1.90	2.15	1.75	1.85	1.84
P_2O_5	1.07	1.01	0.78	0.83	1.08	0.81	0.86	0.83
Sum	99.42	99.67	99.80	100.20	99.58	99.08	99.37	99.40
H_2O^+	0.14	0.19	0.08	0.15	0.21	0.20	0.19	0.10
Rb	56.4	36.6	33.5	36.1	42.4	32.3	35.1	33.8
Sr	1026	1178	1306	1319	1245	1292	1271	1282
Ba	792	601	623	649	692	591	617	616
Sc	5.8		9.9	9.50				
V	17	71	83	71	43	100	90	81
Cr	18	1	0.9	1.9	3	8	2	3
Co	11		17	16.0				
Ni	21	4	8	8	9	9	9	8
Zn	126	130	110	97	115	124	127	113
Ga	23.5	23.0	22.5	24.6	22.4	22.9	23.2	23.3
Y	50	46	44	45	49	43	44	45
Zr	732	535	432	440	553	429	456	443
Nb	76.0	61.3	54.9	55.4	65.3	55.6	59.9	57.6
Hf	15.6		9.5	9.5				
Ta	4.6		3.05	3.25				
Th	6.0		2.7	3.0				
La	75.1		46	47.3				
Ce	184	131	112	118	130	103	114	113
Nd	88		62.5	65.4				
Sm	16.9		13.1	14.1				
Eu	5.02		4.47	4.48				
Tb	1.89		1.76	1.78				
Ho	2.2		1.6	1.6				
Yb	4.18		3.10	3.40				
Lu	0.58		0.43	0.45				

Samples range from hawaiite to mugearite; field locations are designated by solid squares in Figure 5.

[a]Data by XRF

[b]Data by neutron activation

especially diffuse because Hamakua lavas from the windward (high rainfall) coast have lost K_2O during low-temperature alteration. The highest alkali contents are in the Laupahoehoe lavas which define coherent trends of increasing alkalis with MgO decreasing from 4.5 to 2.6%. As in most compositional plots there is a distinct gap between Hamakua and Laupahoehoe lavas and here the Hamakua high Fe-Ti basalts and sample NO-9 occupy an intermediate position.

Compatible trace elements, Cr-Ni-Co: These elements are all positively correlated with MgO and reach very low abundances in the hawaiites and mugearites (Cr <11 ppm and Ni < 12 ppm, except in sample NO-10 which contains dunite xenoliths; Table 1 and Figure 8*b*).

Compatible trace elements, Sc-V: Over the entire MgO range of the Hamakua lavas V abundances increase with decreasing MgO; in contrast, below 7% MgO abundances of Sc and MgO are positively correlated in Hamakua lavas. Laupahoehoe lavas are clearly distinguished by low Sc and V contents, positive trends with MgO content and marked separation from the Hamakua field.

TABLE 1d. Accuracy and Precision Evaluation

	BCR-1[a]	BCR[b]	Precision[c], %
SiO_2	54.66±.51	54.89	0.29
TiO_2	2.23±.10	2.27	0.25
Al_2O_3	13.71±.25	13.57	0.35
Fe_2O_3	13.35±0.46	13.48	0.31
MnO	0.18±0.01	0.19	2.93
CaO	6.99±0.15	6.98	0.23
Na_2O	3.29±0.11	3.17	2.04[d]
Na_2O	-	-	1-2[e]
K_2O	1.70±.08	1.71	0.51
P_2O_5	0.37±.02	0.38	1.68

	BHVO-1[a]	BHVO-1[b]	
Rb	11±2	9.1	2-3
Sr	403±25	390	0-1
Ba	139±14	135	2-3
Sc	31.8±1.3	31.8	1-2
V	317±12	286	1-2
Cr	289±22	289	2-3
Co	45±2	45.1	1-2
Ni	121±2	115	1-3
Zn	105±5	113	1-2
Ga	21±2	21.1	2-4
Y	27.6±1.7	24.6	0-1
Zr	179±21	184	0-1
Nb	19±2	19.7	1-2
Hf	4.38±0.22	4.37	2-3
Ta	1.23±0.13	1.13	3-4
Th	1.08±0.15	0.95	~10
La	15.8±1.3	15.5	1-2
Ce	39±4	39.5	2-3
Nd	25.2±2.0	24.2	3-4
Sm	6.2±0.3	5.93	2-3
Eu	2.06±0.08	2.12	1-2
Tb	0.96±0.08	0.91	7-8
Ho	0.99±0.08		~10
Yb	2.02±0.20	1.96	2-3
Lu	0.29±0.03	0.28	3-4

[a]Consensus literature values with one standard deviation for USGS. standard rock BCR-1 [*Gladney et al.*, 1983] and BHVO-1 [*Gladney and Roelandts*, 1988].

[b]Data for USGS. standard rocks were obtained in this study concurrently with analyses of Mauna Kea samples. Major elements (BCR-1) determined by XRF at University of Massachusetts. Trace element data (BHVO-1) for Sc, Cr, Co, Hf, Ta, Th, and REE are based on nine analyses at MIT (1981-1985); all other trace element data determined by XRF at University of Massachusetts.

[c]Major elements and Rb, Sr, Ba, V, Ni, Zn, Ga, Y, Zr, and Nb precision estimates are 1 standard deviation in percent based on duplicate XRF analyses of all Mauna Kea samples. A typical range is given for these trace elements because precision varies with abundance. Precision estimates for Na_2O (INAA), Sc, Cr, Co, Hf, Ta, Th, and REE are the typical range of 1 standard deviation in percent based on 57 replicate neutron activation analyses of a Hawaiian alkalic basalt and nine replicate neutron activation analyses of BHVO-1. Table 1a also shows mean and deviation of duplicate analyses of NO-13.

[d]XRF

[e]INAA

Incompatible elements. Because P_2O_5 abundance was determined in all lavas and apatite was not an early crystallizing phase in these Mauna Kea lavas (this paper and *West et al.*, [1988]), incompatible trace element abundances are shown as a function of P_2O_5 content (Figure 9). Typically highly incompatible elements such as La, Ce, Nb, Ta, Ba, and Th form coherent positive trends defined by all Mauna Kea lavas with the highest abundances in the Laupahoehoe hawaiites and mugearites. The near-zero intercepts (Figure 9) indicate that all these elements are highly incompatible.

Below ~1%, P_2O_5 abundances of K_2O, Rb and P_2O_5 are positively correlated. However, at higher P_2O_5 contents there is considerable scatter with the mugearite, NO-10, having anomalously high K_2O and Rb contents. Trends for Hamakua lavas show a positive but very scattered trend caused by the atypically low K and Rb contents in Hamakua lavas from the rainy east coast. Hamakua samples from the arid west flank define much more coherent trends. Basaltic samples with <0.2% K_2O, <1 ppm Rb and K/Rb ratios in the range of 1000-3300 have lost most of their original K and Rb. This loss results in bulk rock K_2O/P_2O_5 ratios of less than unity which contrasts with ratios of 1.5-2 in unaltered Hawaiian lavas [e.g., *Wright*, 1971]. Severe alkali metal loss during subaerial alteration of Hawaiian shield lavas was also inferred by *Feigenson et al.* [1983] and *Chen and Frey* [1985]. This interpretation is consistent with detailed compositional studies of alteration profiles on subaerial basalt [*Patterson*, 1971; *Wilson*, 1978].

The K_2O-, Rb- and Ba-P_2O_5 plots include two samples initially collected as Mauna Kea samples (Figure 9*a*). Subsequent mapping showed that they were from Hualalai. These lavas have Rb/P_2O_5 and Ba/P_2O_5 ratios distinct from Mauna Kea lavas thereby illustrating the geochemical differences between these adjacent Hawaiian volcanoes.

Moderately incompatible elements: Zr, Y, Yb, Sr. The Sr-P_2O_5 trend is perhaps the most important trend because it shows opposite slopes for the Hamakua and Laupahoehoe lavas (Figure 9*b*). That is, (1) Hamakua basalts define a positive trend at relatively low Sr and P_2O_5 abundances; (2) the six high Fe-Ti Hamakua lavas also define a positive trend but it is offset from the main Hamakua trend; and (3) the Laupahoehoe lavas have very high Sr contents (>1100 ppm) but define a trend of decreasing Sr with increasing P_2O_5. Clearly, Sr was a compatible element during evolution of the Laupahoehoe Volcanics; an important role for feldspar fractionation is inferred [*cf. West et al.*, 1988].

Abundances of Y and the HREE are positively correlated with P_2O_5, but different slopes are defined by the Laupahoehoe hawaiites/mugearites and Hamakua basalts (Figure 9*b*). Zr and P_2O_5 are also positively correlated in Hamakua and Laupahoehoe lavas, but sample NO-10, a mugearite, lies out of the Laupahoehoe trend (Figure 9b). A possible explanation for the anomalous ratios in sample NO-10 (Figures 9*a* and *b*) is that apatite fractionation has buffered the P_2O_5 content of this sample. This sample contains rare microphenocrysts of olivine, plagioclase, phlogopite, and apatite. As expected from apatite fractionation this mugearite has lower Sm, Eu, and Tb contents than other Laupahoehoe mugearites (cf. NO-10 in Table 1*c* with Mi 1, 3 and 4 in Table 1 of *West et al.* [1988]).

Rare earth elements. All samples have chondrite-normalized LREE/HREE ratios greater than one. In detail, Hamakua basalts, like Hawaiian basalts in general, have steep chondrite-normalized patterns from Eu to Lu with relatively less fractionation from La to Sm; relative to these basalts,

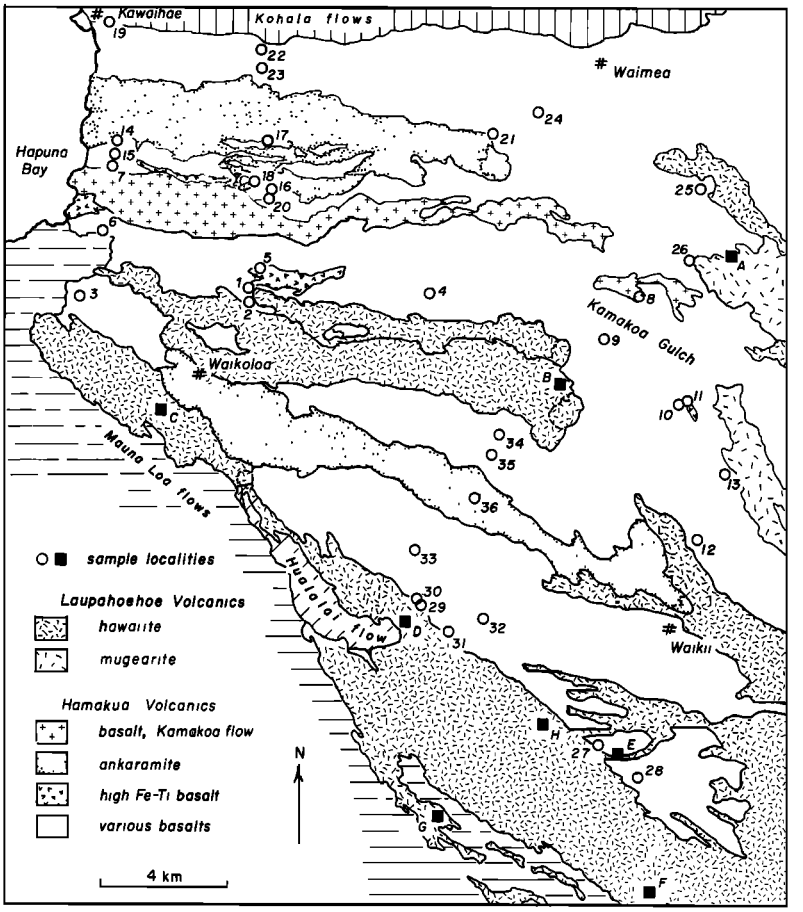

Fig. 5. Geologic map of the northwest flank of Mauna Kea, showing localities of upper Hamakua flows and lower Laupahoehoe flows that were studied (Table 1). The aerial extent of several Hamakua flows is shown.

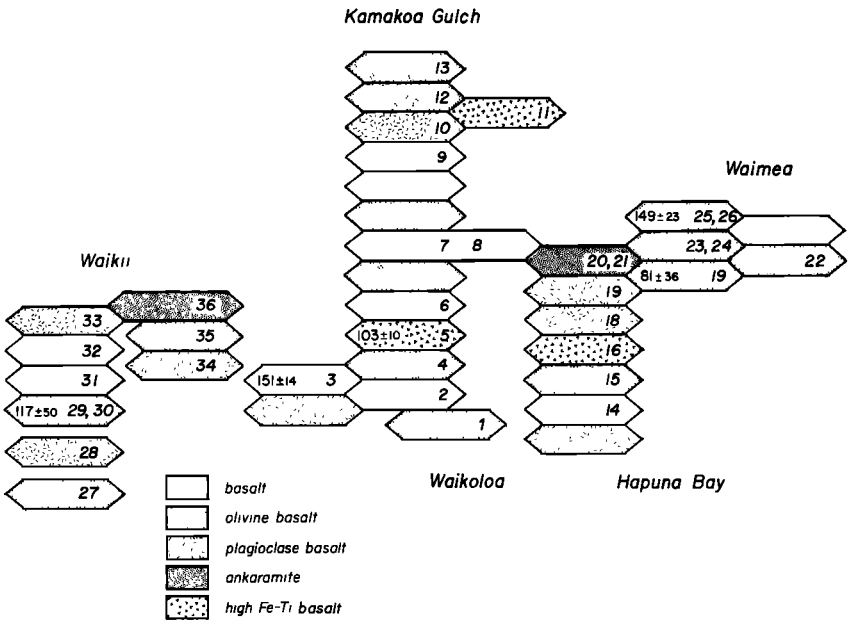

Fig. 6. A diagrammatic representation of the relative ages of the sampled Hamakua flows from the northwest flank of Mauna Kea. Sample numbers correspond to those of Figure 5 and Table 1. Flows labelled basalt contain less than 5% phenocrysts; olivine basalts contain more than 5% olivine phenocrysts; plagioclase basalts contain more than 5% plagioclase (and plagioclase > olivine) phenocrysts; ankaramite contains >30% phenocrysts of olivine and augite; and high Fe-Ti basalts are weakly porphyritic but have Fe_2O_3 contents greater than 15% and TiO_2 greater than 4.5%.

TABLE 2. Selected Mineral Analyses

	Hamakua Samples					Laupahoehoe
	1	5	21	26	32	C
Lava type	olivine basalt	high-Fe-Ti basalt	ankaramite	basalt	olivine basalt	hawaiite
Plagioclase	(ph)[a]	(grd)	(ph)	(mph)	(ph)	(grd)
SiO_2	48.21	52.90	47.82	49.01	47.61	53.54
Al_2O_3	32.97	29.55	33.03	32.40	33.80	29.74
CaO	16.47	11.67	16.41	15.31	17.07	12.04
Na_2O	2.33	5.01	2.35	3.04	2.01	4.83
K_2O	0.12	0.48	0.07	0.12	0.09	0.21
Total	100.11	99.64	99.71	99.91	100.60	100.38
An (%)	79.1	54.7	79.0	72.9	81.9	57.2
Ab (%)	20.2	42.6	20.5	26.3	17.5	41.6
Or (%)	0.7	2.7	0.5	0.8	0.6	1.2
Olivine	(ph)	(grd)	(ph)	(mph)	(ph)	(grd)
SiO_2	40.52	38.11	40.59	40.05	40.35	38.14
FeO	11.64	24.65	13.60	13.73	13.88	25.75
MnO	0.15	0.25	0.16	0.40	0.29	0.45
MgO	46.12	36.12	44.88	44.87	45.32	35.45
CaO	0.34	0.40	0.32	0.28	0.51	0.31
NiO	0.27	0.10	0.22	0.22	0.18	0.09
Total	99.07	99.66	99.80	99.57	100.53	100.21
Fo (%)	86.8	71.6	84.8	84.5	84.3	70.3
Clinopyroxene	(ph)	(grd)	(ph)	(ph)	(ph)	(grd)
SiO_2	52.57	46.03	50.24	45.91	48.48	46.68
TiO_2	0.67	4.02	1.61	2.91	1.85	3.67
Al_2O_3	2.35	4.46	3.62	6.44	4.78	4.40
Cr_2O_3	0.20	0.10	0.10	0.22	0.19	0.05
Fe_2O_3	1.11	4.08	2.33	4.49	3.57	3.97
FeO	4.68	7.19	6.10	4.43	5.28	7.43
MnO	0.15	0.06	0.13	0.16	0.34	0.02
MgO	17.04	11.72	15.20	13.34	14.58	11.53
CaO	21.18	21.50	20.09	21.43	20.48	21.39
Na_2O	0.27	0.62	0.56	0.37	0.37	0.73
Total	100.09	99.87	99.91	99.67	99.75	100.19
Ilmenite	(grd)	(grd)	(grd)	(grd)	-	(grd)
TiO_2	48.69	49.47	49.24	48.59	-	48.28
Al_2O_3	0.36	0.17	0.09	0.33	-	0.47
Fe_2O_3	9.84	7.61	9.09	9.26	-	8.95
FeO	37.09	39.63	38.67	38.08	-	40.34
MnO	0.56	0.62	0.56	0.65	-	0.91
MgO	3.43	2.37	2.83	2.78	-	1.21
Total	99.98	99.87	100.48	99.70	-	100.16
Magnetite	(grd)	(grd)	(grd)	(grd)	(grd)	(grd)
TiO_2	19.06	24.58	19.42	23.30	21.05	23.38
Al_2O_3	1.47	2.10	1.59	0.98	1.93	1.05
Fe_2O_3	31.27	20.03	30.11	23.79	27.13	23.66
FeO	45.71	50.14	46.95	48.85	48.31	48.90
MnO	0.43	0.73	0.56	0.54	0.58	1.08
MgO	1.81	2.14	1.17	2.19	1.41	1.93
Total	99.75	99.73	99.80	99.64	100.41	100.00

Fe_2O_3 was calculated assuming charge balance and stoichiometry.

[a]ph, phenocryst; mph, microphenocryst; grd, groundmass phase.

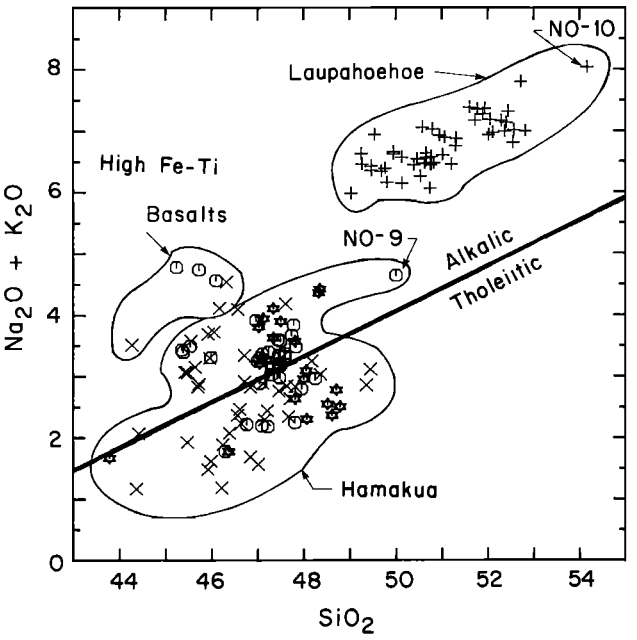

Fig. 7. SiO_2 versus total alkalis (all in wt.%) plot showing data for all Mauna Kea lavas studied. Note the gap between the Hamakua Volcanics (basaltic substage) and Laupahoehoe Volcanics (hawaiite substage). In this and all subsequent compositional diagrams the data include samples from this paper (Table 1) plus Hamakua Volcanics from the east flank (F.A. Frey et al., manuscript in preparation, 1989) and Laupahoehoe Volcanics from the summit and south rift [*West et al.*, 1988]. The Hamakua lavas are subdivided into the arid west flank (hexagon), wet east flank, (cross) and Waikahalulu Gulch (star). These symbols are also used in Figures 8-11. Using the chemical classification scheme of *LeBas et al.* [1986] all Hamakua lavas are basalts and Laupahoehoe lavas range from hawaiite to mugearite.

Laupahoehoe hawaiites and mugearites are enriched in all REE with a higher LREE/HREE ratio (Figure 7 of *West et al.* [1988]).

Radiogenic isotopes, Sr, Nd, Pb. Radiogenic isotope ratios have been measured in 11 lavas of the Laupahoehoe Volcanics and 27 samples of the Hamakua Volcanics including tholeiitic, alkalic, and high Fe-Ti basalts (A.K. Kennedy et al., manuscript in preparation, 1989). Lavas from Laupahoehoe and Hamakua Volcanics overlap in $^{87}Sr/^{86}Sr$ (0.70336 to 0.70362) and $^{143}Nd/^{144}Nd$ (0.51297 to 0.51307) (Figure 10*a*). Although these isotopic variations are larger than analytical error, these isotopic ratios do not vary systematically with relative age. This result contrasts with the systematic temporal variations of Sr and Nd isotopic lavas in postshield lavas (Kula Volcanics) from Haleakala Volcano [*Chen and Frey*, 1985; *West and Leeman*, 1987b]. However, relative to Hamakua lavas, Laupahoehoe lavas trend to lower $^{206}Pb/^{204}Pb$ ratios (Figure 10*b*). Hamakua lavas lie within the field that is characteristic of Hawaiian shield lavas whereas Laupahoehoe lavas overlap with the field for postshield lavas [*Stille et al.*, 1986; *West and Leeman*, 1987b].

5. DISCUSSION: THE POSTSHIELD BASALT TO HAWAIITE TRANSITION

5.1. *Qualitative Constraints Based on Compositional Trends*

The major objective of this paper is to evaluate the petrogenetic relationship between the postshield hawaiite substage (Laupahoehoe Volcanics) and the older postshield basalt substage (Hamakua Volcanics). Three important aspects of these Mauna Kea lavas must be explained: (1) the absence of basalts in the Laupahoehoe Volcanics (Figure 7), (2) the distinct compositional gap between Laupahoehoe lavas and the Hamakua lavas (Figures 7-9), and (3) the generally lower $^{206}Pb/^{204}Pb$ ratios in the Laupahoehoe lavas (Figure 10*b*).

Obviously, the highly evolved Laupahoehoe lavas (MgO <5%, Ni <12 ppm) are not primary melts of typical upper mantle peridotite [e.g., *Maaloe and Aoki*, 1977]. Wilkinson [1985] suggested that hawaiites might be primary melts of an Fe-rich source ($Mg/(Mg+Fe^{+2}) = 0.85$). However, his proposed peridotite source contains 0.43% Cr_2O_3 and 0.23% NiO. It is unlikely that Mauna Kea hawaiites with generally less than 10 ppm Ni and Cr (Table 1*c* and *West et al.* [1988]) can be primary melts because bulk solid/melt partition coefficients >180 are required. (The anomalously high Ni and Cr in the mugearite (NO-10 in Table 1*c*) probably reflect disaggregation of the abundant dunite xenoliths in this flow.)

Consequently, we evaluate the alternative hypothesis that the Laupahoehoe lavas are related to the Hamakua lavas by extensive fractional crystallization. There is strong evidence that crystal fractionation was the major process creating the hawaiite to mugearite compositional trends of Laupahoehoe lavas [*West et al.*, 1988]. Moreover, hawaiites are generally interpreted as forming by fractional crystallization from alkali basalt magmas [e.g., *Macdonald*, 1968; *Vaniman et al.*, 1982]. If the Laupahoehoe lavas were derived from Hamakua basalts, their major and trace element abundance trends (Figures 8 and 9) provide important qualitative constraints on the fractionating mineral assemblage. Specifically, relative to the Hamakua basalts the Laupahoehoe hawaiites and mugearites have (1) higher Al_2O_3/CaO and lower Sc which requires clinopyroxene segregation, (2) higher SiO_2 which requires segregation of SiO_2-poor phases such as olivine and Fe-Ti oxides, (3) very low Ni and Cr content which requires segregation of olivine and pyroxenes, (4) lower FeO* and V which requires segregation of Fe-Ti oxides, and (5) very high Sr contents (1100-1320 ppm) which requires that plagioclase was not a major fractionating phase in the postulated transition from Hamakua basalt to Laupahoehoe hawaiite. For example, the most evolved Hamakua lava contains less than 700 ppm Sr, and the least evolved Laupahoehoe hawaiites contain ~1300 ppm Sr. This subordinate role for plagioclase in the basalt to hawaiite transition contrasts with a major role for plagioclase in the fractionation assemblage required to explain the compositional variations within the Laupahoehoe lavas [*West et al.*, 1988].

All Laupahoehoe lavas are enriched in incompatible elements relative to Hamakua basalts (Figure 9). Abundance ratios, such as Sr/X (where X is a highly incompatible element), are useful in identifying possible parental compositions, and the petrogenetic processes leading to the Laupahoehoe hawaiites. Variations in Sr/X define distinct

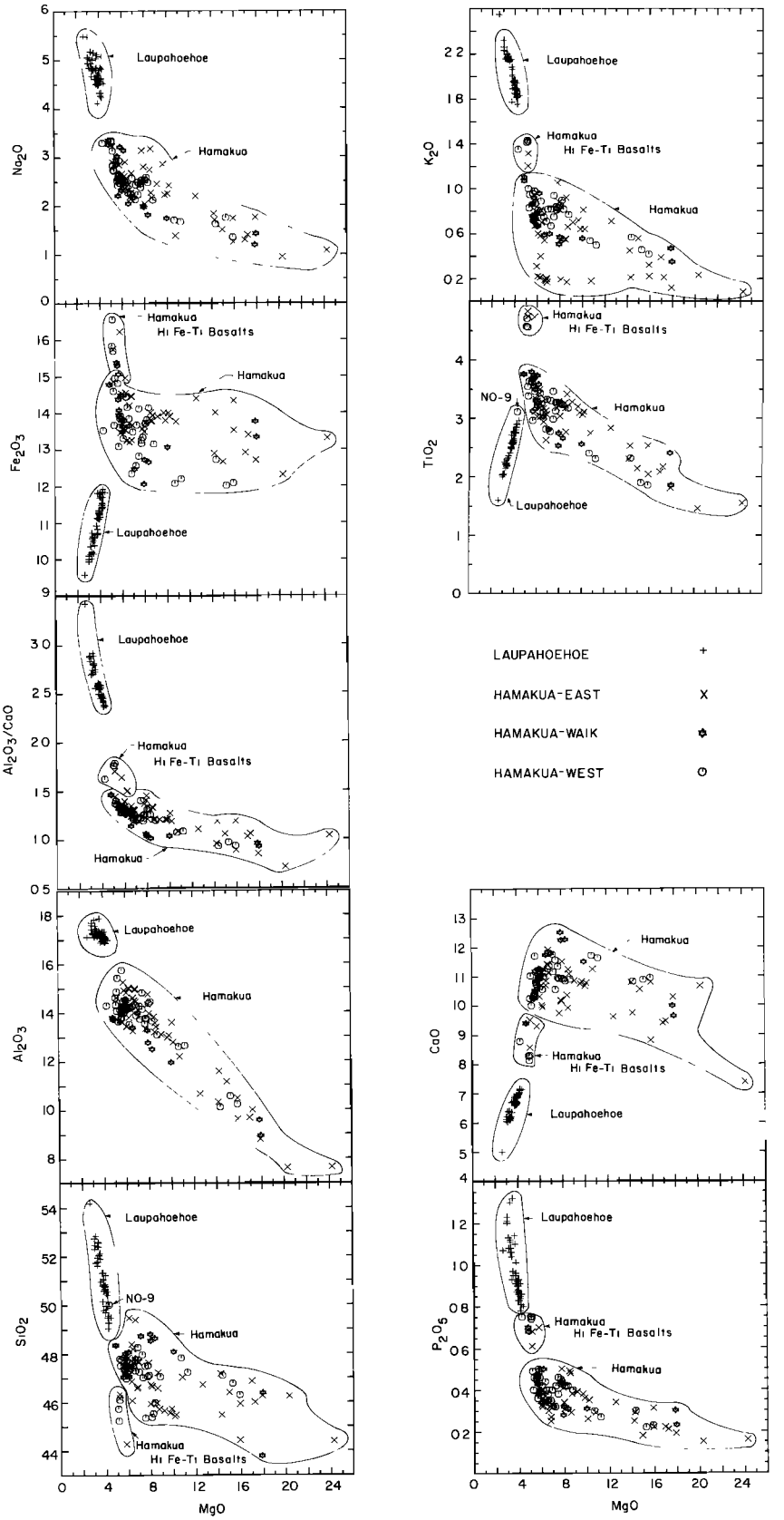

Fig. 8*a*. MgO variation diagrams for major oxides (wt.%). The compositional gap and distinct fields formed by Hamakua and Laupahoehoe lavas are obvious. The field for the Hamakua high Fe-Ti basalt is intermediate in some plots (K_2O, P_2O_5, CaO) but not in others (Fe_2O_3, SiO_2, TiO_2).

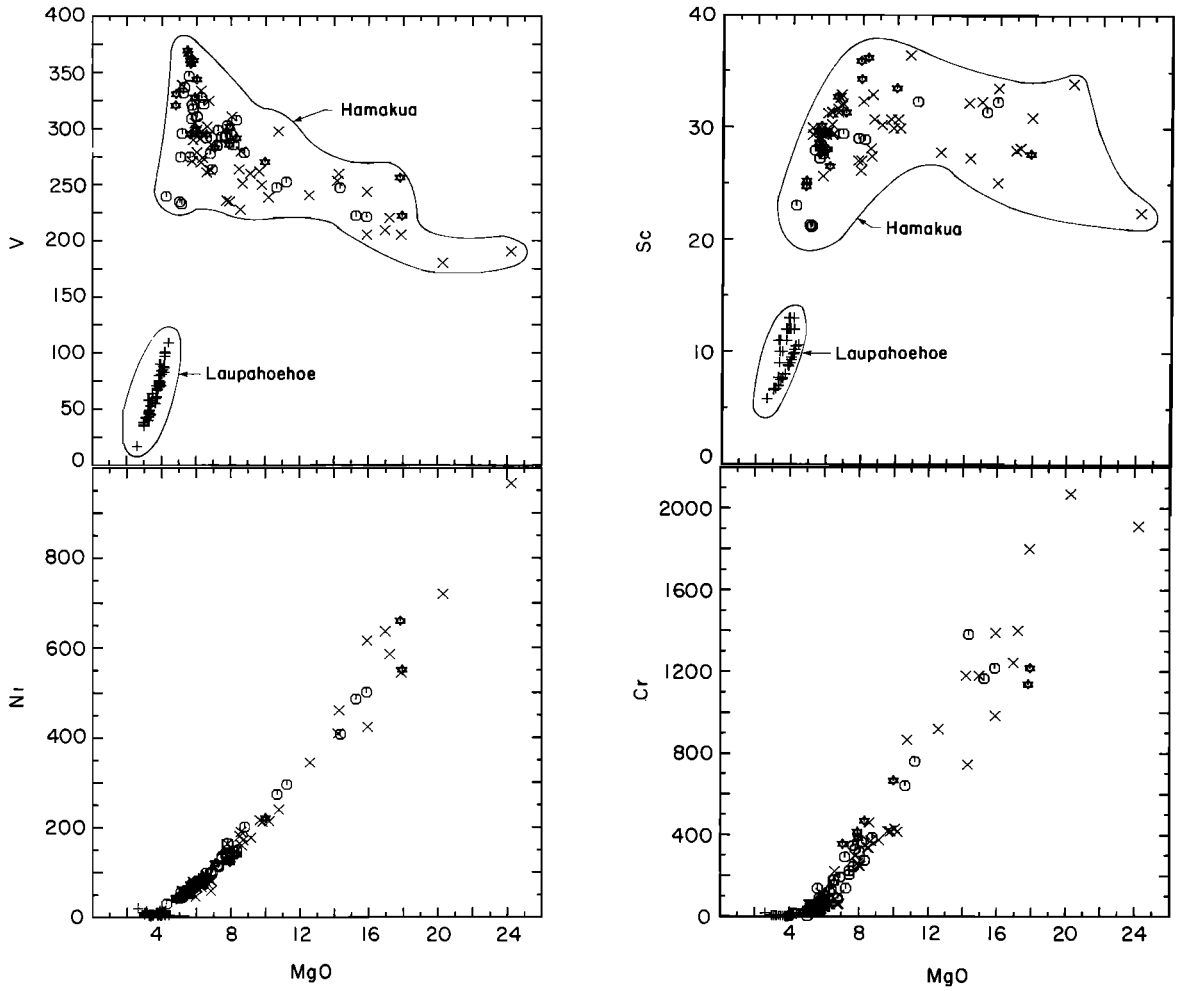

Fig. 8*b*. Ni, Cr, V, and Sc contents (ppm) versus MgO content (wt.%) for Mauna Kea lavas.

but subparallel paths for Hamakua and Laupahoehoe lavas (Figure 11*a*). In both cases the most evolved lavas (lowest MgO) lie at the low Sr/*X* end of the trend. Decreases in Sr/*X* ratios within basic lava suites result from plagioclase fractionation. The well-defined trend of the Laupahoehoe lavas suggests a common parental composition for these hawaiites and confirms the important role for feldspar dominated fractionation in creating the hawaiite to mugearite compositional variation [*West et al.*, 1988]. The trend defined by Hamakua lavas is more scattered, probably because Hamakua samples include accumulative rocks, such as ankaramites and picrites. Accumulation of olivine and pyroxene in a melt will decrease incompatible element contents without changing the Sr/*X* ratio. Scatter within the Hamakua field in Figure 11*a* also results from the presence of basalts whose parents were derived by different degrees of melting (i.e., tholeiitic and alkalic basalts, (F.A. Frey et al., unpublished manuscript, 1989)). Because it is not possible to increase Sr/Ce in residual melts by segregation of feldspar and mafic phases, parental basalts for Laupahoehoe hawaiites had Sr/*X* ratios equal to or greater than the most mafic hawaiite (Figure 11*a*). Moreover, in order to relate Laupahoehoe hawaiites to a Hamakua basalt, a fractionation process is required which increases incompatible element contents without causing a significant decrease in Sr/*X* ratios. Fractionation of mafic phases, such as olivine and clinopyroxene, without a major role for feldspar, is a suitable process (Figure 11*b*).

Clinopyroxene fractionation within the upper mantle and lower crust is apparently an important process in the evolution of alkalic basalts [e.g., *Duda and Schmincke*, 1985]. Moreover, *Knutson and Green* [1975] and *Thompson* [1974] proposed that some continental hawaiites were generated by clinopyroxene-dominated fractionation at moderate pressures (5-10 kbar). Early experimental studies on basaltic systems by *Green and Ringwood* [1967] showed that with increasing pressure, clinopyroxene replaces olivine as the liquidus phase. The recent 1-atm and 8-kbar experimental study of mildly alkalic basalt by *Mahood and Baker* [1986] documents the transition from olivine and plagioclase as early crystallizing phases at 1 atm to clinopyroxene as the liquidus phase at 8 kbar. Therefore a possible qualitative explanation for the origin of the Laupahoehoe hawaiites is fractional crystallization of alkalic

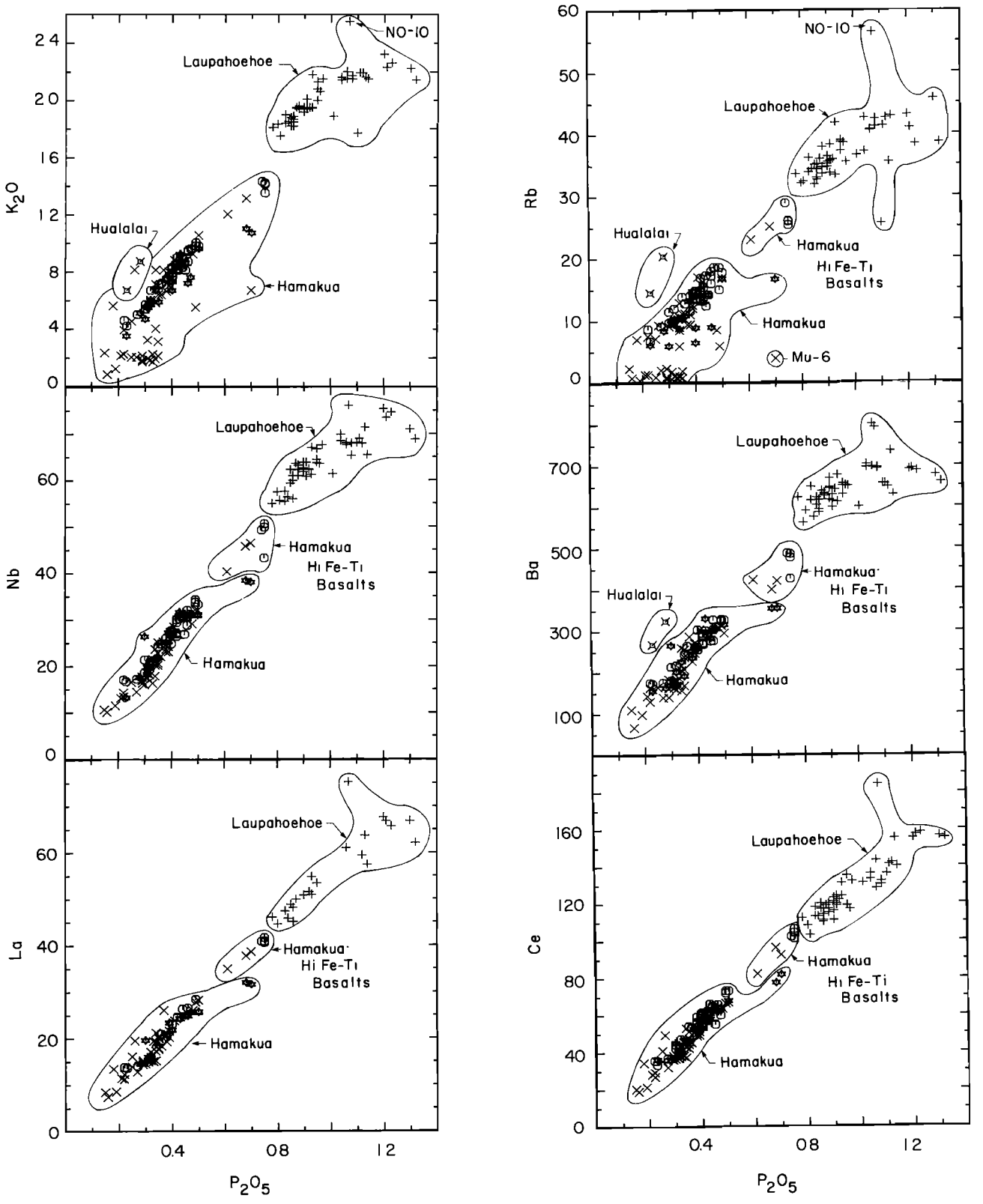

Fig. 9*a*. Abundances of the highly incompatible elements, K (as K_2O in wt.%), Rb, Nb, Ba, La, and Ce (ppm) versus P_2O_5 (wt.%) for Mauna Kea lavas. In contrast to some of the major and compatible element plots (Figure 8), there is a near continuous trend formed by Hamakua and Laupahoehoe lavas. Hamakua lavas with the highest incompatible element content are the six high Fe-Ti basalts, sample NO-9 from the west flank and samples H17 and H17B from the upper part of Waikahalulu Gulch. The high Fe-Ti basalt Mu-6 from the east flank has anomalously low K_2O and Rb because of alteration. Also shown are two Hualalai samples, originally believed to be Mauna Kea lavas, which have distinctly higher K_2O/P_2O_5, Rb/P_2O_5, and Ba/P_2O_5 than Mauna Kea lavas.

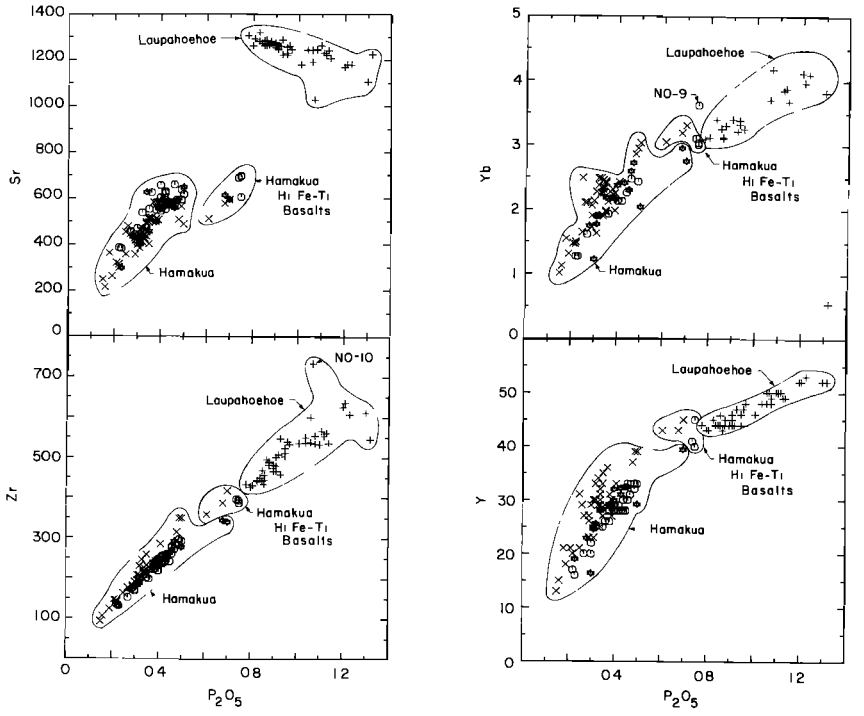

Fig. 9*b*. Abundances of Zr, Y, Yb, and Sr (ppm) versus P_2O_5 (wt.%) for Mauna Kea lavas.

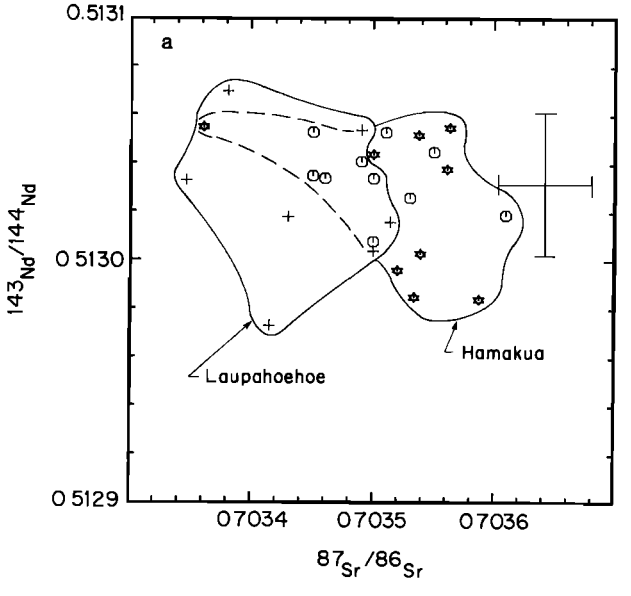

Fig. 10*a*. $^{87}Sr/^{86}Sr$ versus $^{143}Nd/^{144}Nd$. The data vary slightly beyond analytical errors (indicated by ±2 sigma error bars); however, Hamakua and Laupahoehoe lavas overlap in $^{87}Sr/^{86}Sr$ and $^{143}Nd/^{144}Nd$ ratios.

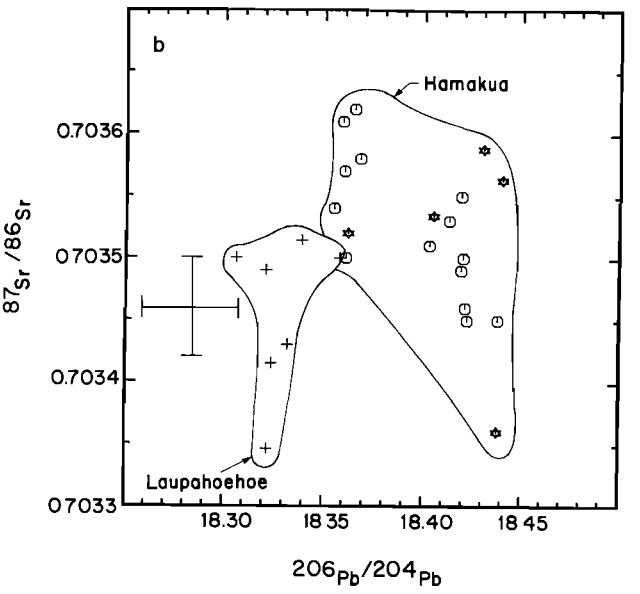

Fig. 10*b*. $^{87}Sr/^{86}Sr$ versus $^{206}Pb/^{204}Pb$ for Mauna Kea lavas. Laupahoehoe lavas extend to slightly lower $^{206}Pb/^{204}Pb$ isotopic ratios than the Hamakua lavas. All data from A. Kennedy et al., manuscript in preparation, 1989.

basalt magmas at pressures where the amount of clinopyroxene exceeds plagioclase in the fractionating assemblage.

5.2. *Constraints Based on Experimentally Determined Liquid Lines of Descent*

The relationships between Hamakua basalts and Laupahoehoe hawaiites can also be evaluated by comparing major element abundances with experimentally determined liquid lines of descent. For example, phase relationships in the tetrahedron, plagioclase, olivine, diopside, and silica have been useful in understanding the evolution of tholeiitic basalts [e.g., *Walker et al.*, 1979; *Tormey et al.*, 1987]. In the projection from plagioclase, Laupahoehoe lavas straddle the clinopyroxene-olivine boundary forming an elongated trend displaced from the 1-atm three-phase saturated field

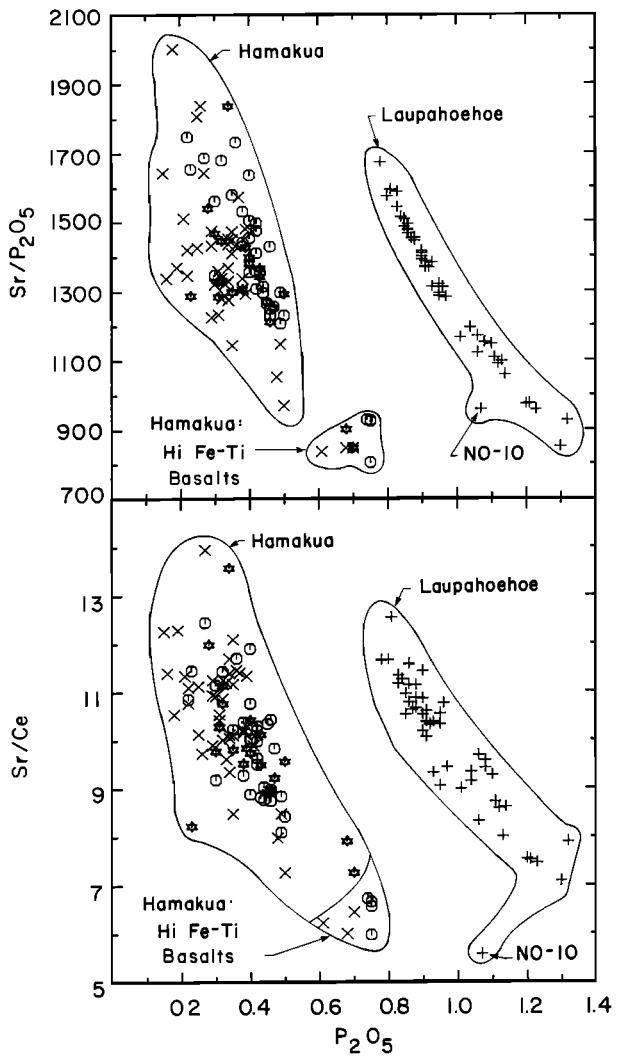

Fig. 11*a*. Sr/P_2O_5 and Sr/Ce versus P_2O_5 (wt.%) for Mauna Kea lavas. There are two subparallel trends: a well defined trend for the Laupahoehoe lavas (hawaiites and mugearite) and a broader trend defined by the Hamakua lavas (tholeiitic, alkalic, and high Fe-Ti basalts, picrites, ankaramites).

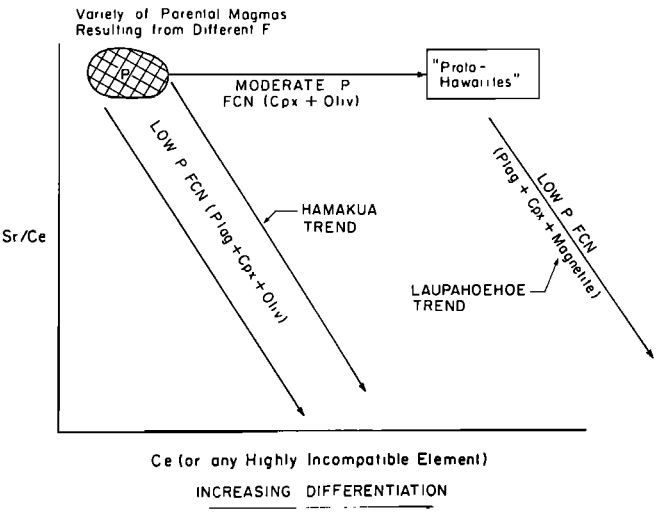

Fig. 11*b*. Interpretative diagram for Figure 11*a*. The two subparallel trends reflect varying Sr/Ce which is caused by fractionation of a plagioclase-rich assemblage. Apparently, these two relatively low pressure trends emanate from different parental melts which are indicated by the rectangle labelled "Proto-Hawaiites" and the cross-hatched field labelled P which designates basalts derived by different degrees of melting (F). The coherent trend for the Laupahoehoe lavas reflects derivation from a compositionally homogeneous parental melt. Compared to Hamakua lavas this parental melt ("Proto-Hawaiites") for the Laupahoehoe Volcanics has a higher incompatible element content but similar Sr/Ce; i.e., both Sr and Ce were incompatible during formation of the "Proto-Hawaiites." Therefore the transition from Hamakua basalt to Proto-Hawaiite requires fractionation of a clinopyroxene + olivine, plagioclase-poor assemblage. The labels LOW or MODERATE P FCN indicate the relative pressure of fractional crystallization. The fractionating mineral assemblage is listed for each trend in parenthesis.

toward higher normative olivine (Figure 12*a*). These hawaiites are also rich in plagioclase (Figure 12*b*, ~71% normative feldspar). The scatter of the Hamakua field in Figure 12 reflects the diverse magma types, tholeiitic and alkalic, plus picritic and ankaramitic accumulates (F.A. Frey et al., unpublished manuscript, 1989). Nevertheless, many of the Hamakua basalts lie within the region of three-phase saturation at 1 atm. Therefore a major distinction between the Laupahoehoe lavas and Hamakua basalts is that the Laupahoehoe hawaiites and mugearites are substantially displaced from low-pressure cotectics.

A more appropriate system for alkalic lavas is the tetrahedron, diopside, olivine, plagioclase, and nepheline [*Sack et al.*, 1987]. In the plane diopside-olivine-nepheline, the Hamakua lavas define a very diverse field with tholeiites most distant from the nepheline apex, ankaramites, and picrites closest to the olivine apex and alkalic lavas nearest the experimentally determined field for three-phase (olivine, clinopyroxene, and plagioclase) saturated melts at 1 atm (Figure 13*a*). In contrast, Laupahoehoe lavas define a coherent elongated array which is not near the 1-atm, three-phase saturated cotectic (Figure 13*a*). *Sack et al.* [1987] showed that with increasing pressure, the three-phase saturated cotectics move toward the olivine apex. Thus the trend defined by Laupahoehoe lavas is consistent with moderate pressure fractionation. Apparently, many of the Hamakua lavas reflect a lower-pressure fractionation history than the Laupahoehoe lavas.

Because Laupahoehoe lavas dominantly consist of a plagioclase component, it also is important to project their compositions onto a plane including plagioclase. For example, Laupahoehoe lavas and Hamakua ankaramites-picrites overlap in the Di-Ol-Ne subprojection (Figure 13*a*), but they are clearly separated in the Pl-Ol-Di subprojection (Figure 13*b*). Within the hawaiite field the liquid line of descent is toward the plagioclase apex; e.g., the most evolved mugearite (NO-10) lies at the plagioclase-rich end of the field.

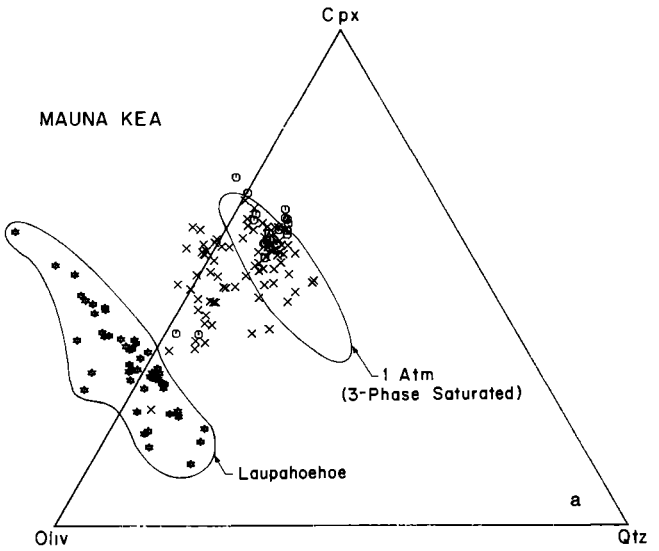

Fig. 12*a*. Projection of Laupahoehoe and Hamakua lavas onto the clinopyroxene-quartz-olivine plane (projected from plagioclase following the convention of *Tormey et al.*, [1987]). Hamakua data indicated by cross (east and west flanks) and circle (Waikahalulu Gulch); Laupahoehoe data indicated by stars. Note the coherent trend defined by the Laupahoehoe lavas which lie closer to the olivine apex than most Hamakua lavas. Only a few Hamakua picrites lie within Laupahoehoe field. The hawaiites and mugearites do not plot near the trend defined by three phase (oliv-plag-cpx) saturated low P cotectics (field based on data for MORBs from *Walker et al.*, [1979], *Grove and Bryan* [1983], and *Tormey et al.* [1987]).

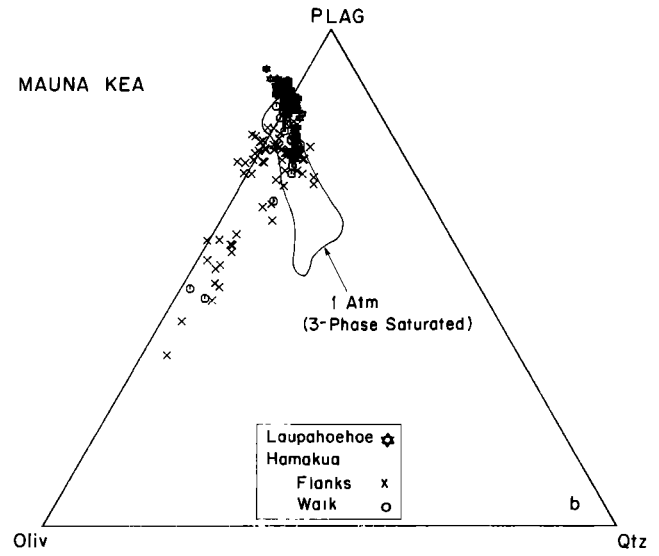

Fig. 12*b*. Projection of Laupahoehoe and Hamakua lavas on the plane olivine-plagioclase-quartz (projected from clinopyroxene). The Laupahoehoe field is displaced to high plagioclase contents with the most evolved Laupahoehoe lavas having the largest plagioclase content.

Although the Laupahoehoe lavas are displaced from the 1-atm three-phase saturated field in Figure 13*b*, enrichment of the plagioclase component with increasing differentiation characterizes both the 1-atm experimental data and the Laupahoehoe lavas.

Based on comparisons of Mauna Kea lava compositions with three-phase saturated, low pressure liquid lines of descent (Figures 12 and 13), we conclude that Laupahoehoe lavas were not formed at low pressures within an upper crustal magma chamber. Moreover, most Hamakua basalts reflect low-pressure fractionation processes that did not affect the hawaiites and mugearites; therefore most Hamakua basalts are not suitable as parents for Laupahoehoe lavas. Based on Figure 13*a*, the most suitable parental compositions for Laupahoehoe lavas are (1) Hamakua ankaramites and picrites which overlap with or lie to the high pressure side of the Laupahoehoe field or (2) a few Hamakua basalts which are close to the Laupahoehoe field.

5.3. *Quantitative Evaluation of an Equilibrium Crystallization Model Based on Major Elements*

Although a single-step, least squares model for major element variation from basalt to hawaiite is at best a gross approximation, it is important to determine if this simple process can explain major and trace element abundance trends. In order to quantitatively evaluate an equilibrium crystallization model for the Laupahoehoe hawaiites we chose to model sample Mi-5, the most mafic hawaiite found by *West et al.* [1988], as a residual melt from partial crystallization of a more mafic parent. Criteria for choosing possible parental magmas include major element compositions (Figure 13*a*) and Sr/*X* ratios (Figure 11). In addition, we did not consider MgO-rich rocks that are probably accumulates rather than crystallized melts (e.g., $Al_2O_3/CaO<0.9$ reflects accumulative clinopyroxene, (F.A. Frey et al., manuscript in preparation, 1989)). With these criteria, several Hamakua lavas were evaluated as possible parental magmas. In the Di-Ol-Ne subprojection (Figure 13*a*), only Hamakua ankaramites overlap with the Laupahoehoe field. Therefore we evaluated ankaramites 97-14 and 115-12 as possible parents for Laupahoehoe lavas. These ankaramites have suitable Sr/Ce (11-11.5), but they have lower Al_2O_3/CaO (0.93-0.97) than most Mauna Kea basalts (Table 1). In addition, we also evaluated as possible parents a picrite (LP-6, 16.6% MgO, $Al_2O_3/CaO = 1.19$) and three alkalic basalts (MU-5, KI-2, and LP-9) all from the east flank (F.A. Frey et al., manuscript in preparation, 1989). These basalts have $Al_2O_3/CaO = 1.19$ to 1.41 and slightly higher Diop/Oliv ratios than the Laupahoehoe field in Figure 13*a*.

Mineral compositions in equilibrium with Mi-5 were estimated using constraints from K_D values for Fe/Mg in olivine and Na/Ca in plagioclase (Table 3*a*). Clinopyroxene phenocrysts are absent in Laupahoehoe hawaiites; therefore experimental studies were used to estimate clinopyroxene compositions (Table 3*a*). Segregation of a gabbroic mineral assemblage was evaluated because the major element trends clearly require segregation of olivine, clinopyroxene, and plagioclase; also, gabbroic xenoliths, interpreted as cumulate in origin, are common in some Laupahoehoe lavas [*Fodor and Vandermeyden*, 1988].

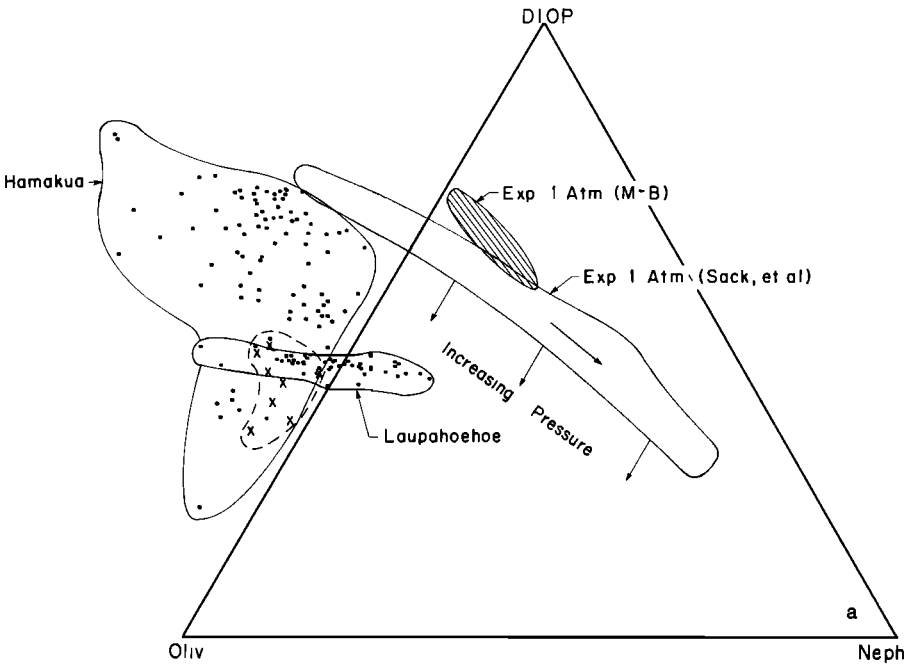

Fig. 13*a*. Projection of Laupahoehoe and Hamakua lavas onto the diopside-nepheline-olivine plane (projected from plagioclase following the convention of *Sack et al.* [1987]). The fields labeled "Exp. 1 Atm." enclose melt compositions that are saturated with olivine, clinopyroxene, and plagioclase at low pressure (data from *Sack et al.* [1987] and *Mahood and Barker* [1986]. Arrow within shaded field indicates trend of increasing fractionation. *Sack et al.* [1987, Figure 12] showed that with increasing pressure these cotectics move toward the olivine apex. Note that the Laupahoehoe lavas define a coherent trend displaced well away from the 1-atm cotectic. Hamakua lavas, tholeiitic and alkalic basalts plus picrites and ankaramites form a scattered field primarily to the low-pressure side of the Laupahoehoe trend. Hamakua lavas that might be parental to Laupahoehoe lavas are indicated by x's within the dashed field. The alkalic basalts, Mu-5, Ki-2, and Lp-9 were also evaluated as possible parents (Table 3), but they are just above the dashed field at higher diop/oliv ratios.

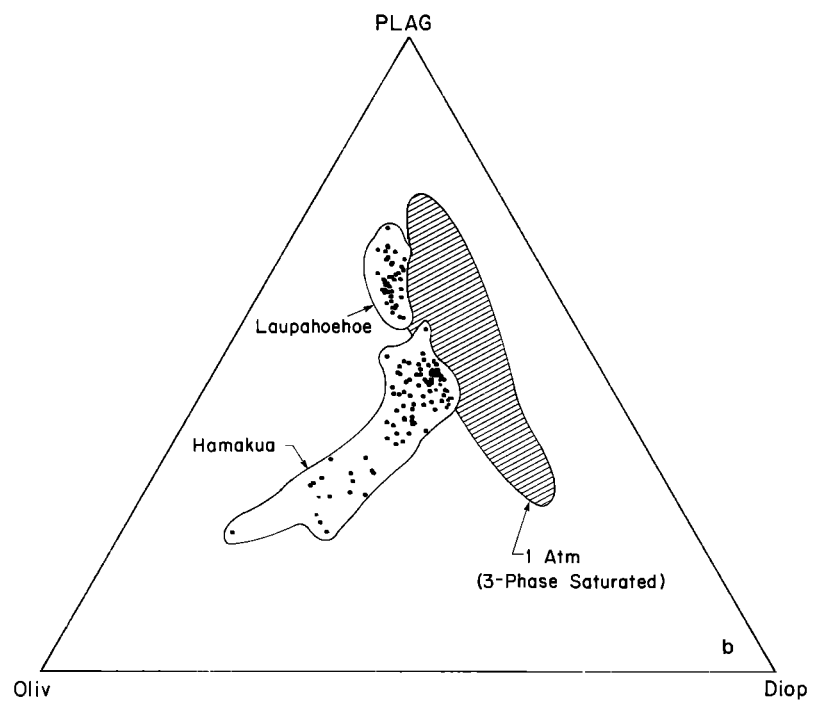

Fig. 13*b*. Projection of Laupahoehoe and Hamakua lavas on the olivine-diopside-plagioclase plane (projected from nepheline following the convention of *Sack et al.* [1987]. There is no overlap of the lava groups, and the plagioclase-rich nature of Laupahoehoe lavas is illustrated.

TABLE 3a. Crystallization Models for Deriving Laupahoehoe Hawaiite Mi-5 as a Residual Melt From Hamakua Lavas: Mineral Compositions (Estimated to be in Equilibrium With Mi-5) Used in Models

	Olivine[a]	Plagioclase[b]	Clinopyroxene[c]	Oxides[d]	Oxides[e]
SiO_2	37.71	53.4	48.36	-	-
TiO_2	-	-	2.24	16.89	51.1
Al_2O_3	-	29.65	8.56	3.13	0.17
FeO	24.16	0.65	6.80	67.47	42.22
MgO	37.75	-	13.31	5.89	4.86
CaO	-	11.56	20	-	-
Na_2O	-	4.26	0.73	-	-
K_2O	-	0.24	-	-	-

[a]$Fo_{73.6}$, groundmass olivine in Mi-5, K_D = 0.31 [*West et al.*, 1988].

[b]$An_{59.1}$, microphenocryst in Mi-5, K_DCa/Na= 1.72 [*West et al.*, 1988].

[c]Estimated equilibrium composition using constraints from experimental studies [e.g., *Mahood and Baker*,1986]; K_DFe/Mg=0.25, D_{TiO_2}=0.75, $D_{Al_2O_3}$=0.5, D_{Na_2O}=0.16.

[d]Microphenocryst in Mi-5 [*West et al.*, 1988].

[e]Ilmenite not found in Laupahoehoe lavas. This analysis from ilmenite in an evolved Hamakua lava (F.A. Frey et al., manuscript in preparation, 1989).

TABLE 3b. Results for Crystal Segregation Models for Deriving

	Residual Melt[a]	Alkalic Basalts as Parents[b]						
	Observed	MU-5		KI-2		LP-9		
	Hawaiite Mi-5	Observed	Gabbroic Model	Observed	Gabbroic Model	Observed	Gabbroic Model	Wherlite Model[d]
SiO_2	49.97	46.85	46.52	46.20	45.91	46.08	46.00	46.13
TiO_2	2.98	3.35	3.34	3.16	3.15	3.24	3.24	2.18
Al_2O_3	17.15	14.61	14.60	12.98	12.98	13.12	13.12	12.39
FeO	10.76	12.38	12.27	12.71	12.61	12.74	12.71	11.76
MgO	4.47	8.09	7.95	10.36	10.24	9.77	9.70	9.20
CaO	7.22	10.38	10.36	10.94	10.92	10.86	10.82	10.82
Na_2O	4.57	2.86	3.04	2.46	2.56	2.88	2.67	2.74
K_2O	1.84	0.90	0.99	0.65	0.80	0.73	0.87	1.06
Σr_2			0.18		0.14		0.08	3.06
								Fractionation
Olivine			4.60		9.27		7.71	2.22
Plagioclase			10.77		9.00		7.39	
Clinopyroxene			26.71		34.17		33.09	31.62
Oxides (ilm+mt) in gabbro model, cr-spinel in wherlite model			5.66		5.36		5.49	8.67
Residual melt (Mi-5)			52.27		42.20		46.32	57.49
1/F (F=residual melt fraction)			1.91		2.37		2.16	1.74

[a]Mi-5 is the most mafic Laupahoehoe hawaiite studied by *West et al.* [1988].

[b]Alkalic basalts (KI-2 and LP-9) and picrite (LP-6) are from gulches on the east coast of Mauna Kea which expose the oldest available subaerial Hamakua lavas (F.A. Frey et al., manuscript in preparation, 1989)

[c]Ankaramite 97-14 is a Hamakua lava (see Figures 5 and 6 and Table 1).

[d]Wherlite model uses olivine as in Table 3a and cpx and Cr-spinel data for a wherlite xenolith (T. Atwill and M. Garcia, unpublished data, 1987).

[e]Fe-Ti oxides are included in the first column but excluded in the second column.

These compositionally diverse (alkalic basalt, ankaramite, and picrite) Hamakua lavas have major element compositions which can yield hawaiite compositions by segregation of a gabbroic assemblage (Table 3*b*). Parental alkalic basalts can generate hawaiite melts with ~4.5% MgO by ~50% subtraction, of a clinopyroxene-rich (~60%) gabbroic mineral assemblage containing 10-16% olivine, 13-23% plagioclase, and ~10% Fe-Ti oxides (Table 3b). Although the olivine gabbro xenoliths in Laupahoehoe lavas have a wide range of modal proportions most are dominated by clinopyroxene (40-68 vol.%) with significant olivine and plagioclase [*Fodor and Vandermeyden*, 1988, Table 1]. Because Sr must be an incompatible element in the transition from basalt to hawaiite, we attempted to minimize the role of feldspar in these models. However, eliminating plagioclase in the gabbroic accumulate results in unsatisfactory models ($\Sigma r^2 > 0.57$). We also evaluated segregation of a wherlite assemblage (olivine, clinopyroxene, and Cr-spinel) because dunite and wherlite xenoliths also occur in Laupahoehoe hawaiites [*Jackson et al.*, 1982]. However, wherlite models are unsuccessful (Table 3*b*).

The ankaramites are also suitable as parents for Laupahoehoe lavas. Again a gabbroic mineral assemblage provides the most satisfactory model. If Fe-Ti oxides are excluded from the model, the fractionating assemblage (~75% crystallization) contains ~60% clinopyroxene, 30% olivine, and 10% plagioclase (Table 3*b*). Although the role of segregating olivine is increased for picritic parents, such as LP-6, clinopyroxene is also required as a major component, ~40%, of the segregating assemblage (Table 3*b*). Therefore, based on major oxide contents, the best models involve segregation of a clinopyroxene-rich gabbroic mineral assemblage from Hamakua lavas to form residual Laupahoehoe hawaiites. This conclusion is consistent with the moderate pressure (8 kbar) experimental results of *Mahood and Baker* [1986].

These mass balance models are simplistic and do not provide unique solutions. However, if Laupahoehoe lavas were derived as residual melts from parental Hamakua lavas, these models identify the fractionating minerals required and provide approximate estimates of their proportions. As a test of models based on major elements, incompatible element enrichments, i.e., (Laupahoehoe hawaiite)/(possible Hamakua parents), are compared to the maximum values, expected from major element models (i.e., $1/F$ in Table 3*b*). These comparisons (Figure 14) eliminate some Hamakua lavas as

Laupahoehoe Hawaiite, Mi-5, From Hamakua Parental Lavas

Ankaramite Parent[c]							Picrite Parent[b]		
97-14				115-12			LP-6		
Observed	Gabbroic Models[e]		Wherlite Model[d]	Observed	Gabbroic Models[e]		Observed	Gabbroic Model	Wherlite Model[d]
47.00	46.86	46.60	47.34	47.39	47.14	46.81	45.44	45.24	45.64
1.89	1.89	1.63	1.58	1.92	1.92	1.72	2.59	2.59	1.70
10.38	10.39	10.51	8.82	10.71	10.72	10.85	10.71	10.73	9.61
11.04	11.00	11.37	12.45	10.96	10.88	11.78	13.20	13.14	13.66
16.12	16.10	16.00	14.94	15.45	15.40	15.32	16.26	16.20	15.40
11.12	11.15	11.31	10.81	11.02	11.05	11.19	9.02	9.03	8.86
1.62	1.83	1.78	2.06	1.68	1.98	1.92	1.95	2.02	2.23
0.43	0.49	0.44	0.77	0.47	0.57	0.52	0.33	0.57	0.86
	0.07	0.43	6.44		0.17	0.61		0.11	3.37
Assemblage (wt.%)									
	25.06	24.67	4.14		23.19	22.97		29.23	22.78
	8.33	9.97	36.88		7.20	9.23		10.99	
	41.66	42.56			40.16	40.90		28.15	26.05
	-0.70		4.47		-0.83			2.56	4.49
	25.65	22.81	42.08		30.29	26.90		29.49	46.68
	3.90	4.38	2.38		3.30	3.72		3.39	2.14

possible parents for the most mafic Laupahoehoe hawaiite; e.g., basalt LP-9 is too depleted in the highly incompatible elements (Th through Sr). In contrast, incompatible element abundances in alkali basalt MU-5 are much more consistent with the fractionation model based on major elements; only small, 5-10%, discrepancies occur for K, Nb, Sr and P (Figure 14). Except for K, Rb, and Th the incompatible element abunances in the picrite and ankaramites are also consistent with the major element models (Figure 14). In these comparisons, little weight should be given to mismatches for K and Rb because of their mobility during alteration and to Th in picrites and ankaramites because of large analytical errors at <1 ppm Th.

There are several likely reasons for the deficiencies of models using Hamakua alkalic basalts as parents for Laupahoehoe lavas: (1) these basalts have an overprint of low-pressure fractionation that is inadequately accounted for by simple models; (2) the slightly lower $^{206}Pb/^{204}Pb$ in the Laupahoehoe lavas (Figure 10*b*) requires addition of a component with relatively low $^{206}Pb/^{204}Pb$, perhaps a wallrock component that was also enriched in incompatible elements; and (3) the spectrum of Hamakua alkalic to tholeiitic basalts probably reflects a range in degree of melting and we may not have identified the most suitable parental basalt. Also, the coherent geochemical trends defined by the Laupahoehoe lavas are consistent with derivation from a common parental hawaiite composition (Figures 8 and 9). It is important that our Hamakua to Laupahoehoe models consider the least evolved Laupahoehoe lava. In this regard, our unpublished data for a Laupahoehoe hawaiite (W86, H6-206 (E.W. Wolfe et al., submitted manuscript, 1989)) with 4.74% MgO yields results very similar to models for hawaiite Mi-5 (4.45% MgO) in Table 3*b* and Figure 14.

In summary, we can not realistically model the large compositional gap between MgO-rich Hamakua lavas and Laupahoehoe hawaiites. However, some Hamakua lavas have major and trace element compositions that are suitable as parents for Laupahoehoe lavas. Thus it is plausible that Laupahoehoe hawaiites were derived from Hamakua parents by melt-mineral segregation involving clinopyroxene as the major (40-60%) fractionating phase with accompanying plagioclase (10-20%), and olivine (10-40%) and possibly lesser amounts of Fe-Ti oxides. In the subsequent section we couple this clinopyroxene-dominated fractionation model with geological and physical constraints to formulate a volcano evolution model which can explain the absence of basalts in the Laupahoehoe Volcanics, the distinct compositional gap between the Hamakua and Laupahoehoe lavas, and the lower $^{206}Pb/^{204}Pb$ ratios in Laupahoehoe lavas.

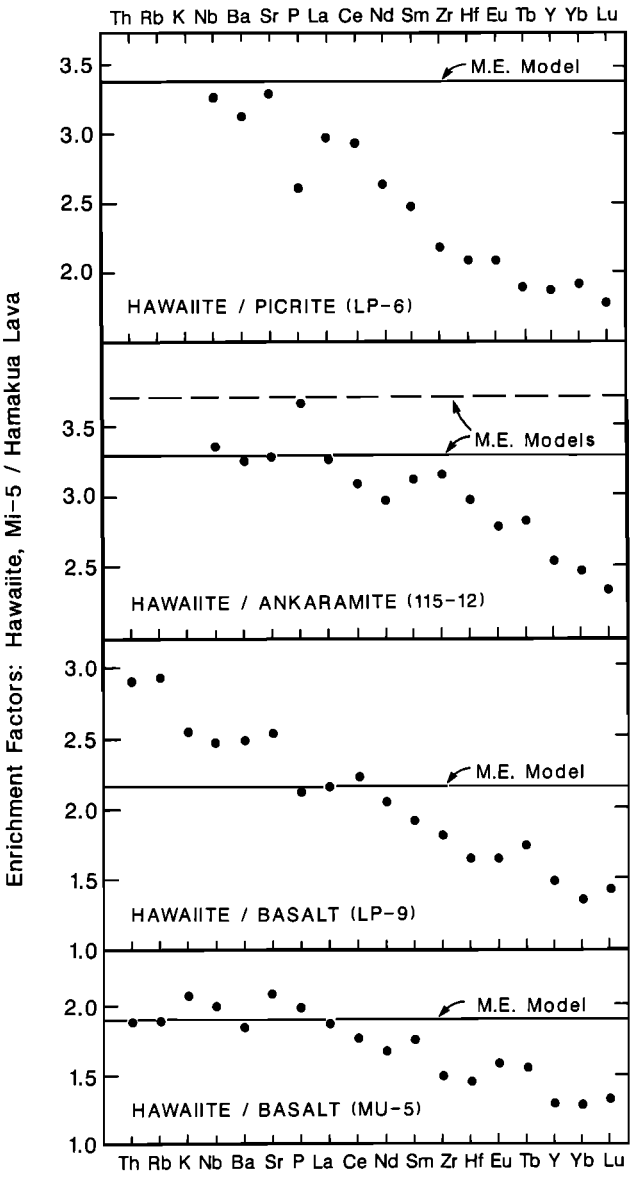

Fig. 14. Trace element enrichment factors calculated from comparing abundances in Laupahoehoe hawaiite Mi-5 to the Hamakua lavas which yielded permissible major element models (Table 3*b*). Elements are arranged in a general order of decreasing enrichment. This order is similar to that typically used in normalized incompatible element plots for oceanic basalts except that Sr and P are more commonly plotted near Nd. Note that Sr and Nb were highly incompatible reflecting a minor role for feldspar and oxide segregation, respectively; this contrasts with the Laupahoehoe hawaiite to mugearite trends where Sr and Nb are more compatible than LREE [cf. Figure 11 of *West et al.*, 1988]. The solid lines labeled M.E. Model indicate the maximum incompatible element enrichments possible for the major element models (i.e., 1/F in Table 3*b*). Dashed line in panel for 115-12 is for segregation of an oxide-free assemblage. Points lying above these horizontal lines (e.g. Th-Sr in LP-9) reflect inconsistencies between the simple major element models and incompatible element abundance. Some models, i.e., MU-5 and 115-12, can satisfactorily explain ME and most of the incompatible element contents. Th, Rb, and K data points are not plotted for the picrite and ankaramite because these samples lost alkalis during low temperature alteration and the Th data are imprecise at these abundance levels (<1 ppm).

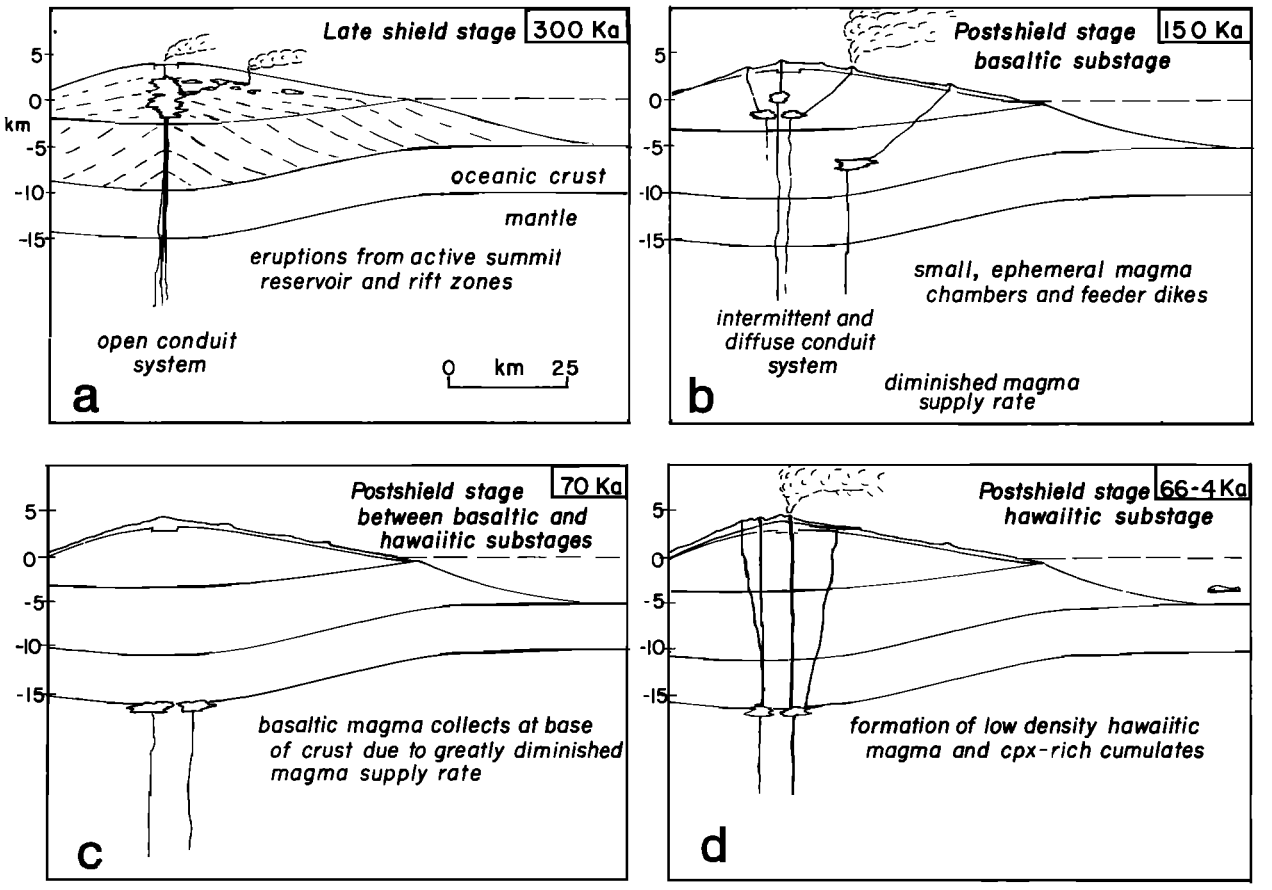

Fig. 15. Generalized east-west cross section showing volcanic plumbing of Mauna Kea volcano as a function of time. (a) Late shield stage (~300 ka). Magma supply rate is sufficient to maintain open conduits to a continuously replenished shallow magma chamber system. Eruptions occur at the summit and along rift zones. (b) Postshield basaltic substage (Hamakua Volcanics, ~150 ka). Magma supply rates have decreased reflecting a decrease in degree of melting leading to eruption of alkalic basalts with radiogenic isotope ratios similar to the tholeiitic basalts. Magma chambers are not continuously replenished and high Fe-Ti basalts form as residual melts in cooling, isolated chambers within the shallow crust (F.A. Frey et al., manuscript in preparation, 1989). Conduits supply magma to summit and flank vents. (c) Postshield stage (~70 ka) at the transition between the basaltic and hawaiitic substages. Magma supply rates have decreased substantially (Figure 1). Shallow magma chambers and crustal conduits have crystallized because the magma supply rate is insufficient to maintain open fractures for magma ascent through the crust. Basaltic magma now ponds at the oceanic crust-mantle interface because there is insufficient driving force for ascent through the lower-density crust. These magmas cool, dense minerals form and assimilation of wall rock can occur. (d) Postshield hawaiite substage (Laupahoehoe Volcanics, ~66-4 ka). Magma supply rates continue to decrease. Low-density residual melts segregate from a dense clinopyroxene-rich accumulate. The low-density hawaiite and mugearite melts have sufficient buoyancy to open new ascent fractures. Eruptions are not confined to the summit and rift zones. During ascent, further crystallization of a plagioclase-rich accumulate may occur on conduit walls, and the magmas incorporate xenoliths of gabbro, dunite, and wherlite.

6. DISCUSSION: POSTSHIELD EVOLUTION OF MAUNA KEA VOLCANO

In the following discussion, interpretations of the Hamakua-Laupahoehoe geochemical trends are used to develop a physical model for evolution of Mauna Kea volcano. A summary model for the late shield and postshield evolution of Mauna Kea volcano is presented in Figure 15.

During the shield building stage melt production rate in the mantle is high, leading to rapid volcano growth (Figure 1) and establishment of a shallow magma chamber such as that currently beneath the summits of Kilauea and Mauna Loa (Figure 15*a* and *Ryan et al.* [1981]; *Lockwood et al.* [1987]; *Klein et al.* [1987]). Termination of the shield building stage is caused by a significant decrease in eruption rate, presumably reflecting a decrease in melt production within the mantle. For example, relative to the growth rates during the shield building stage, growth rates during the basaltic substage of postshield volcanism are lower by factors of 3-15 (Figure 1). F.A. Frey et al. (manuscript in preparation, 1989) concluded that this decrease in melt production has several important consequences: (1) Melts formed over a

range in degree of melting can be segregated and erupted, resulting in isotopically similar intercalated tholeiitic and alkalic basalt lavas; (2) Shallow magma chambers cool and crystallize significantly before replenishment by basaltic magma (Figure 15*b*). These episodes of extensive fractionation led to the high Fe-Ti basalts which occur in the upper part of the Hamakua Volcanics. Probably, some of the olivine gabbro xenoliths in the Laupahoehoe lavas [*Fodor and Vandermeyden*, 1988] formed at shallow levels during this process. .

At Mauna Kea (also, Kohala [see *Spengler and Garcia*, 1988]) there is an abrupt termination to the eruption of basaltic lavas. We hypothesize that the decreased melt supply was insufficient to maintain the fractures which enabled basaltic magmas to ascend into shallow crustal magma chambers [e.g., *Spera*, 1984; *Ten Brink and Brocher*, 1987]. Consequently, basaltic magma ponded at some depth, perhaps the lower crust-upper mantle boundary (Figure 15*c*). As the late-stage basaltic lavas cooled at moderate pressures, crystallization was dominated by clinopyroxene (~50%) with significant amounts of olivine, plagioclase and Fe-Ti oxides (Figure 15*d*).

Segregation of melt from dense minerals had important consequences. Specifically, melt density decreased from ~2.73 g/cm^3 for Hamakua basalt to <2.67 g/cm^3 for Laupahoehoe hawaiites and mugearites (on an anhydrous basis, Figure 16). Assuming the parental alkalic basalt melt contained ~0.8% water [Byers et al., 1985], the ~50% fractionation required to create hawaiites leads to ~1.6% water. This volatile enrichment would enhance the predicted density difference between basaltic (~2.70) and hawaiitic (<2.61) melts. The distinct compositional gap between Hamakua and Laupahoehoe lavas (Figures. 6-9 and 11) may have formed because eruption was not possible until a sufficient density difference between wall rocks and residual melt was achieved. That is, the relatively dense basaltic lavas characteristic of the basaltic substage were not able to erupt or even replenish shallow magma chambers because greatly diminished magma production rates led to solidification of the crustal plumbing system. However, with extensive segregation of dense minerals at moderate pressures, e.g., at the crust-mantle boundary, density differences between the evolved residual magma and wall rock became sufficient to enable renewed eruption but only of evolved, low- density hawaiite magmas (Figure 15d).

At low volatile contents, eruption of hawaiitic lavas might be hindered by their high viscosity, ~1 x 10^4 Poises. The factor of 2 increase in water content caused by fractionation is sufficient to decrease the viscosity to ~1 x 10^3, which is much closer to that of the alkalic basalts, ~1 x 10^2. The importance of density and viscosity changes with melt composition during fractional crystallization was previously emphasized by *Stolper and Walker* [1980], who postulated that these changes may be an explanation for compositional gaps in suites of genetically related lavas.

Thompson [1972] proposed that a compositional gap between basaltic and associated lavas with higher SiO_2 contents reflects cooling of stagnated, small, and irregularly shaped magma batches within the lower crust. During the first ~50% of crystallization, no segregation of melt and crystals occurs. Eventually, a crystal meshwork is formed which can fracture, thereby enabling evolved interstitial melt

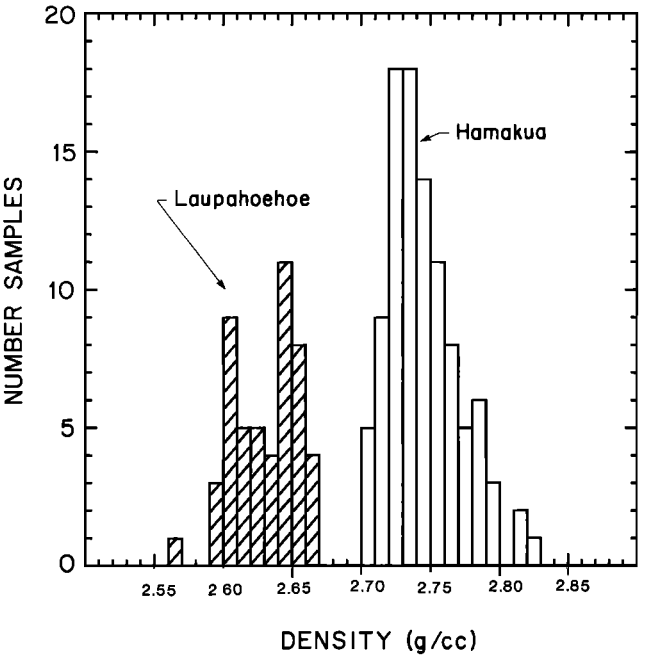

Fig. 16. Histogram of anhydrous melt density for Laupahoehoe and Hamakua lavas. Even the highly evolved Hamakua lavas (e.g., sample NO-9, 4.26% MgO and the high Fe-Ti basalts, ~5% MgO) have densities greater than 2.70; i.e., significantly higher than that of Laupahoehoe lavas (<2.66). Densities calculated at 1000°C for hawaiites and mugearites, 1100°C for Hamakua lavas with <6% MgO, and 1200°C for Hamakua lavas with >6% MgO. In all case, Fe^{3+}/Fe^{2+} was adjusted to the QFM buffer [*Kilinc et al.*, 1983]. Partial molar volumes from *Stebbins et al.* [1984]. If the hawaiites formed at higher temperatures than 1000°C and with higher volatile contents than the basalts, the density differences between Laupahoehoe hawaiites/mugearites and Hamakua basalts would be larger than shown.

(Laupahoehoe lavas) to escape and erupt. This model enhanced by a decreased supply of basaltic magma and the lower density of residual hawaiitic melts may be a general explanation of the abrupt basalt to hawaiite transition at Mauna Kea and Kohala volcanoes. Moreover, it provides an explanation for the nearly aphyric nature of Laupahoehoe lavas.

Finally, ponding of basaltic magma at the lower crust-upper mantle boundary could result in assimilation of MORB-related wall rocks, thereby explaining the trend to lower $^{206}Pb/^{204}Pb$ in the hawaiite substage lavas (Figure 10*b*). *West and Leeman* [1987*b*] proposed this process for explaining isotopic trends among postshield lavas from Haleakala volcano.

7. DISCUSSION: COMPARISON OF POSTSHIELD LAVAS FROM MAUNA KEA, KOHALA, HUALALAI AND HALEAKALA

In this section, postshield lavas from Mauna Kea, Kohala, Hualalai, and Haleakala are compared in order to evaluate the generality of the postshield petrogenetic processes inferred for Mauna Kea volcano.

The postshield stages at Mauna Kea and Kohala, the adjacent and slightly older volcano (Figure 2), have many important similarities,

1. The youngest postshield lavas are exclusively evolved lavas; i.e., the hawaiite substage is composed dominantly of hawaiites with lesser amounts of more evolved lavas [*Lanphere and Frey*, 1987; *Spengler and Garcia*, 1988; *West et al.*, 1988].

2. There is a compositional gap between the hawaiites and the underlying basalts, but this abrupt transition occurred over a small time interval (<30 ka) [this paper; *Spengler and Garcia*, 1988].

3. Relative to underlying basalts, the hawaiitic lavas have high Al_2O_3/CaO, low Sc, and high Sr contents. Therefore, if the hawaiites are related to basalts by crystal fractionation, a clinopyroxene-rich, plagioclase-poor cumulate is required [this paper; *Feigenson et al.*, 1983; *Spengler and Garcia*, 1988].

4. Hawaiite substage lavas are nearly aphyric (<1% phenocrysts) and compositional variations between these lavas require fractionation of a plagioclase-rich assemblage containing significant amounts of clinopyroxene and Fe-Ti oxides [*West et al.*, 1988; *Spengler and Garcia*, 1988].

5. Radiogenic isotope ratios within hawaiite substage lavas range slightly beyond analytical precision, but these small variations do not correlate with lava composition or age [West et al., 1988; *Spengler and Garcia*, 1988].

Because of these similarities, the hawaiite substage lavas at both volcanoes probably formed by similar processes; that is, crystal-melt segregation, at moderate pressures where clinopyroxene is near the liquidus, was the major process in generating the parental magma of the hawaiite substage.

However, there are also important differences between hawaiite substage lavas on Mauna Kea and Kohala. These provide additional constraints on the transition from basaltic substage to hawaiitic substage.

1. Hawaiite substage lavas at Kohala have lower $^{87}Sr/^{86}Sr$ than most of the older basaltic lavas [*Hofmann et al.*, 1987; *Lanphere and Frey*, 1987]. Although at Kohala this $^{87}Sr/^{86}Sr$ difference is small, this result contrasts with the more extensive overlap among Mauna Kea lavas (Figure 10). Lower $^{87}Sr/^{86}Sr$ in hawaiite substage lavas may reflect assimilation of MORB-related wall rocks during moderate pressure fractionation. If the moderate pressure magma chamber at each volcano existed at different depths and temperatures for varying times, differences in the amount of wallrock interaction are expected.

2. The hawaiite substage at Kohala contains a higher proportion of highly evolved lavas, such as mugearites, benmoreites and trachyte [*Spengler and Garcia*, 1988]. The larger proportion of more evolved lava types in the hawaiite substage of Kohala requires more extensive fractionation, either during ascent in conduits or in small magma chambers. This more extensive fractionation may have facilitated increased wall rock interaction which created the $^{87}Sr/^{86}Sr$ contrast between the basalts and the evolved lavas.

3. Kohala hawaiite substage lavas contain apatite (0.1-0.3%), and relative to Mauna Kea hawaiites they have much higher P_2O_5 and higher REE contents, especially higher middle REE [see Figure 13 of *Spengler and Garcia*, 1988]. Relative to basalts, Kohala hawaiites have very high P_2O_5/Ce (>110 for hawaiites with >3.4% MgO [*Spengler and Garcia*, 1988]. Therefore *Spengler and Garcia* [1988] concluded that Kohala hawaiites are not residual liquids formed by closed system fractional crystallization of underlying alkalic basalts with similar Sr and Nd isotopic ratios. They concluded that the high P_2O_5/Ce ratios in Kohala hawaiites require derivation from or contamination by an apatite-rich source.

In contrast, to the abrupt transition from basalt to evolved lavas at Kohala and Mauna Kea, postshield lavas (0.36-0.86 Ma) at Haleakala consist of several repetitive alkali basalt to hawaiite/mugearite sequences [*Chen and Frey*, 1985; *West and Leeman*, 1987*a*], and there is no compositional gap between the basalts and more evolved lavas [*Chen et al.*, manuscript submitted, 1989). Also, there is significant isotopic diversity ($^{87}Sr/^{86}Sr$ from 0.70308 to 0.70346) within the postshield lavas of Haleakala (34 samples analyzed by *Chen and Frey* [1985] and *West and Leeman* [1987*b*]). *West and Leeman* [1987*a*] concluded that the crystal fractionation process from basalt to hawaiite/mugearite at Haleakala was accompanied by mixing in recharged magma chambers. This conclusion is compatible with eruption of alkalic basalt with varying radiogenic isotopic ratios throughout the postshield stage at Haleakala, and the absence of a compositional gap between the basalts and more evolved lavas (C.Y. Chen et al., manuscript submitted 1989). Thus an important feature of Haleakala volcano is that a fracture system enabling basaltic eruptions existed throughout the postshield stage. Similarly at Hualalai volcano, young (<15 ka) basaltic postshield lavas postdate earlier (100-105 ka) postshield eruptions of trachyte [Clague, 1987*b*].

In summary, postshield lavas have been studied at four Hawaiian volcanoes. The eruption rate of basaltic volcanism diminishes during this stage because magma production rates in the mantle decrease substantially. At Mauna Kea and Kohala, basaltic magmas cooled at moderate pressures and fractionated to produce evolved lavas, the hawaiite substage. However, at each volcano differences in volcanic plumbing and magma supply rate led to different proportions of basalt and evolved lava during the postshield stage, and varying degrees of interaction with MORB-related wall rocks.

8. SUMMARY

The transition from shield to postshield volcanism at Hawaiian volcanoes results from a rapid decrease in volcano growth rate; volcano growth and eruption rates continue to decrease during postshield volcanism (Figure 1). At Mauna Kea volcano, postshield volcanism can be divided into two substages; a basaltic substage, ~240-70 ka, (Hamakua Volcanics) and a hawaiitic substage, 66-4 ka (Laupahoehoe Volcanics). There is a distinct compositional gap between these substages. Major and trace element abundances are broadly consistent with segregation of a clinopyroxene-rich (>50%) mineral assemblage from Hamakua basalts to form Laupahoehoe hawaiites. This mineralogy contrasts with the plagioclase-dominated cumulate required to explain compositional trends within the hawaiite substage [*West et al.*, 1988]. The important role for clinopyroxene segregation in the transition from basalt to hawaiite is consistent with mineral-melt fractionation at moderate pressures [e.g., *Green*

and Ringwood, 1967; *Thompson*, 1974; *Mahood and Baker*, 1986].

The compositional gap between the substages was created when magma production rates were insufficient to maintain conduits for ascent of basaltic magma. Consequently, basaltic magma ponded at depth, perhaps at the mantle-oceanic crust boundary. During cooling, clinopyroxene was a major crystallizing phase accompanied by olivine, plagioclase, and Fe-Ti oxides. Segregation of this dense assemblage created low-density hawaiitic magmas. These hawaiitic lavas were sufficiently buoyant to erupt and form the hawaiite substage which contains no basaltic lavas. This model is outlined in Figure 15.

This moderate pressure origin for lavas forming the hawaiite substage is based on compositional trends for the lavas. However, this interpretation is consistent with models based on xenoliths in Hawaiian lavas. Specifically, hawaiite substage lavas at Mauna Kea contain dense xenoliths of dunite, wherlite, olivine gabbro and opaque oxide-rich gabbros [*Jackson et al.*, 1982; *Fodor and Vandermeyden*, 1988], and postshield alkalic basalts from Hualalai contain xenoliths such as dunite, wherlite, websterite and cumulate-textured gabbros [*Jackson et al.*, 1981]. *Clague* [1987*a*,*b*] inferred the depths of magma chambers during volcano growth by postulating that magma reservoirs act as hydraulic filters that remove relatively dense xenoliths from ascending magma. Therefore, the minimum equilibrium pressure of xenoliths reflects the shallowest possible magma reservoir for the host lava. Clague [1987*a*,*b*] interpreted that some xenoliths in postshield lavas equilibrated at depths >19 km. Consequently, he inferred that postshield lavas erupt from magma chambers at ~20 km, considerably deeper than the 3-7 km depth magma chambers present during shield building. Thus inferences based on equilibration pressures of included xenoliths are consistent with petrogenetic inferences based on geochemical data for postshield lavas.

Acknowledgments. We thank S.R. Hart and G. Tilton for access to mass spectrometry facilities; J.M. Rhodes for access to X ray fluorescence, P. Ila for neutron activation analyses, M. Baker for providing a computer program for calculating melt density and viscosity, and C.-Y. Chen for help with sample preparation. We have benefitted from discussions with M. Baker, D. Clague, and T. Grove and manuscript reviews by D. Clague, T. Grove, D. Presnall, and J.M. Rhodes. Nuclear irradations were made at the MIT nuclear reactor. Research was supported by NSF grants EAR 8218982, EAR 8419723, and EAR 875809 to F.F. and EAR 8026787 and OCE 8416216 to M.G. Hawaii Institute of Geophysics contribution 2190.

REFERENCES

Bacon, C.R., and M.M. Hirschmann, Mg/Mn partitioning as a test for equilibrium between coexisting Fe-Ti oxides, *Am. Mineral.*, *73*, 57-61, 1988.

Budahn, J.R., and R.A. Schmitt, Petrogenetic modeling of Hawaiian tholeiitic basalts: A geochemical approach, *Geochim. Cosmochim. Acta*, *49*, 67-87, 1985.

Byers, C.D., M.O. Garcia, and D.W. Muenow, Volatiles in pillow rim glasses from Loihi and Kilauea volcanoes, Hawaii, *Geochim. Cosmochim. Acta*, *49*, 1887-1896, 1985.

Chen, C.-Y., and F.A. Frey, Origin of Hawaiian tholeiites and alkalic basalt, *Nature*, *302*, 785-789, 1983.

Chen, C.-Y., and F.A. Frey, Trace element and isotopic geochemistry of lavas from Haleakala volcano, East Maui, Hawaii: Implications for the origin of Hawaiian basalts, *J. Geophys. Res.*, *90*, 8743-8768, 1985.

Chen, C.-Y., F.A. Frey, S.R. Hart, and M.O. Garcia, Isotopic and rare-earth element geochemistry of the transition from tholeiitic to alkalic volcanism in the Haleakala volcano, East Maui, *Eos Trans. AGU*, *66*, 1133, 1985.

Christofferson, E., The relationship of sea-floor spreading in the Pacific to the origin of the Emperor Seamounts and the Hawaiian Island Chain (abstract), *Eos Trans. AGU*, *49*, p. 214, 1968.

Clague, D.A., Hawaiian alkaline volcanism, in Alkaline Igneous Rocks, (edited by J.G. Fitton, and B.G.J. Upton) *Geol. Soc. London Spec. Publ.*, *30*, 227-252, 1987*a*.

Clague, D.A., Hawaiian xenolith populations, magma supply rates, and development of magma chambers, *Bull. Volcanol.*, *49*, 577-587, 1987*b*.

Clague, D.A., and G.B. Dalrymple, The Hawaiian-Emperor Volcanic Chain, part 1, Geologic evolution, *U.S. Geol. Surv. Prof. Pap. 1350*, pp. 5-54, 1987.

Coombs, D.S., and J.F.G. Wilkinson, Lineages and fractionation trends in undersaturated volcanic rocks from the East Otago volcanic province (New Zealand) and related rocks, *J. Petrol.*, *10*, 440-501, 1969.

Duda, A., and H.-U. Schmincke, Polybaric differentiation of alkalic basaltic magmas: Evidence from green-core clinopyroxenes (Eifel, F.R.G.), *Contrib. Mineral. Petrol.*, *91*, 340-353, 1985.

Dzurisin, D., R.Y. Koyanagi, and T.T. English, Magma supply and storage at Kilauea Volcano, Hawaii, 1956-1983, *J. Volcanol. Geotherm. Res.*, *21*, 177-206, 1984.

Feigenson, M.D., Constraints on the origin of Hawaiian lavas, *J. Geophys. Res.*, *91*, 9383-9393, 1986.

Feigenson, M.D., A.W. Hofmann, and F.J. Spera, Case studies on the origin of basalt, II, The transition from tholeiitic to alkalic volcanism on Kohala volcano, Hawaii, *Contrib. Mineral. Petrol.*, *84*, 390-405, 1983.

Fodor, R.V., and H.J. Vandermeyden, Petrology of gabbroic xenoliths from Mauna Kea Volcano, Hawaii, *J. Geophys. Res.*, *93*, 4435-4452, 1988.

Frey, F.A., and M.F. Roden, The mantle source for the Hawaiian Islands: Constraints from the lavas and ultramafic inclusions, in *Mantle Metasomatism*, edited by M.A. Menzies and C.J. Hawkesworth, pp. 423-463, Academic, San Diego, Calif., 1987.

Gladney, E.S., C.E. Burns and I. Roelandts, 1982 Compilation of elemental concentrations in eleven United States Geological Survey rock standards, *Geostandards Newsletter*, *7*, 3-226, 1983.

Gladney, E.S., and I. Roelandts, 1987 Compilation of elemental concentration data for USGS BHVO-1, MAG-1, QLO-1, RGM-1, SCO-1, SDC-1, SGR-1 and STM-1, *Geostands. Newsletter*, *12*, 253-362, 1988.

Green, D.H., and A.E. Ringwood, The genesis of basaltic magmas, *Contrib. Mineral. Petrol.*, *15*, 103-190, 1967.

Grove, T.L., and W.B. Bryan, Fractionation of pyroxene-phyric MORB at low pressure: An experimental study, *Contrib. Mineral. Petrol.*, *84*, 293-309, 1983.

Hofmann, A.W., M.D. Feigenson, and I. Raczek, Kohala revisited, *Contrib. Mineral. Petrol.*, *95*, 114-122, 1987.

Ila, P., and F.A. Frey, Utilization of neutron activation analysis in the study of geologic materials, *Atomkernenerg. Kerntect.*, *44*, 710-716, 1984.

Jackson, E.D., D.A. Clague, E. Engleman, W.F. Freisen, and D. Norton, Xenoliths in the alkalic basalt flows of Hualalai Volcano, Hawaii, *U.S. Geol. Surv. Open File Rep.*, *81-1031*, 33 pp., 1981.

Jackson, E.D., M.H. Beeson, and D.A. Clague, Xenoliths in volcanic rocks from Mauna Kea Volcano, Hawaii, *U.S. Geol. Surv. Open File Rep.*, *82-201*, 19 pp., 1982.

Kilinc, A., I.S.E. Carmichael, M.L. Rivers, and R.O. Sack, The ferric-ferrous ratio of natural silicate liquids equilibrated in air, *Contrib. Mineral. Petrol.*, *83*, 136-140, 1983.

Klein, F.W., R.Y. Koyanagi, J.S. Nakata, and W.R. Tanigawa, The seismicity of Kilauea's magma system, *U.S. Geol. Surv. Prof. Pap.*, *1350*, 1019-1185, 1987.

Knutson, J., and T.H. Green, Experimental duplication of a high-pressure megacryst cumulate assemblage in a near-saturated hawaiite, *Contrib. Mineral. Petrol.*, *52*, 121-132, 1975.

Kurz, M.D., M.O. Garcia, F.A. Frey, and P.A. O'Brien, Temporal helium isotopic variation within Hawaiian volcanoes: Basalts from Mauna Loa and Haleakala, *Geochim. Cosmochim. Acta*, *51*, 2905-2914, 1987.

Langenheim, V.A.M., and D.A. Clague, The Hawaiian-Emperor volcanic chain, stratigraphic framework of volcanic rocks of the Hawaiian Islands, *U.S. Geol. Surv. Prop. Pap.*, *1350*, 55-84, 1987.

Lanphere, M. and F.A. Frey, Geochemical evolution of Kohala volcano, Hawaii, *Contrib. Mineral. Petrol.*, *95*, 100-112, 1987.

LeBas, M.J., R.W. LeMaitre, A. Streckeisen, and B. Zanettin, A chemical classification of volcanic rocks based on the total alkali-silica diagram, *J. Petrol.*, *27*, 745-750, 1986.

Lockwood, J.P., and P.W. Lipman, Holocene eruptive history of Mauna Loa Volcano, *U.S. Geol. Surv. Prof. Pap.*, *1350*, pp. 509-535, 1987.

Lockwood, J.P., J.J. Dvorak, T.T. English, R.Y. Koyanagi, A.T. Okamura, M.L. Summers, and W.R. Tanigawa, Mauna Loa 1974-1984: A decade of intrusive and extrusive activity, *U.S. Geol. Surv. Prof. Pap.*, *1350*, 537-570, 1987.

Maaloe, S., and K. Aoki, The major element composition of the upper mantle estimated from the composition of lherzolites, *Contrib. Mineral. Petrol.*, *63*, 161-173,1977.

Macdonald, G.A., Composition and origin of Hawaiian lavas, *Mem. Geol. Soc. Am.*, *116*, 477-522, 1968.

Macdonald, G.A., and T. Katsura, Chemical compositions of Hawaiian lavas, *J. Petrol.*, *5*, 82-133, 1964.

Macdonald, G.A., A.T. Abbott, and D.C. Cox, *Volcanoes in the Sea*, 517 pp., University of Hawaii Press, Honolulu, 1983.

Mahood, G.C., and D.R. Baker, Experimental constraints on depths of fractionation of mildly alkalic basalts and associated felsic rocks: Pantelleria, Strait of Sicily, *Contrib. Mineral. Petrol.*, *93*, 251-264, 1986.

Martinson, D.G., N.G. Pisias, J.D. Hays, J. Imbrie, T.C. Moore, Jr., and N.J. Shackleton, Age dating and the orbital theory of the ice ages: Development of a high-resolution 0-300,000 year chronostratigraphy, *Quat. Res.*, *27*, 1-29, 1987.

Moore, J.G., Subsidence of the Hawaiian Ridge, *U.S. Geol. Surv. Prof. Pap.*, *1350*, 85-100, 1987.

Moore, J.G., and R.S. Fiske, Volcanic substructure inferred from dredge samples and ocean-bottom photographs, Hawaii, *Geol. Soc. Am. Bull.*, *80*, 1191-1202, 1969.

Moore, R.E., D.A. Clague, M. Rubin and W.A. Bohrson, Hualalai Volcano: A preliminary summary of geologic, petrologic and geophysical data, *U.S. Geol. Surv. Prof. Pap.*, 1350, 571-585, 1987.

Morgan, W.J., Plate motions and deep mantle convection, *Mem. Geol. Soc. Am.*, *132*, 7-22, 1972.

Patterson, S.H., Investigations of ferruginous bauxite and other mineral resources on Kauai and a reconnaissance of ferruginous bauxite deposits on Maui, Hawaii, *U.S. Geol. Surv. Prof. Pap.*, *656*, 1971.

Porter, S.C., Quaternary stratigraphy and chronology of Mauna Kea, Hawaii, *Geol. Soc. Am. Bull.*, part II, *90*, 980-1093, 1979.

Rhodes, J.M., Homogeneity of lava flows; chemical data for historic Mauna Loan eruptions, *Proc. Lunar Planet. Sci. Conf. 13th*, Part 2, *J. Geophys. Res.*, *88*, suppl., A869-A879, 1983.

Ryan, M.P., R.Y. Koyanagi, and R.S. Fiske, Modelling the three-dimensional structure of macroscopic magma transport systems: Application to Kilauea Volcano, Hawaii, *J. Geophys. Res.*, *86*, 7111-7129, 1981.

Sack, R.O., D. Walker, and I.S.E. Carmichael, Experimental petrology of alkalic lavas: Constraints on cotectics of multiple saturation in natural basic liquids, *Contrib. Mineral. Petrol.*, *96*, 1-23, 1987.

Shaw, H.R., Viscosities of magmatic silicate liquids: An empirical method of prediction, *Am. J. Sci.*, *272*, 870-893, 1972.

Spengler, S.R., and M.O. Garcia, Geochemistry of the Hawi Lavas, Kohala Volcano, Hawaii, *Contrib. Mineral. Petrol.*, *99*, 90-104, 1988.

Spera, F.J., Carbon dioxide in petrogenesis, III, Role of volatiles in the ascent of alkaline magma with special reference to xenolith-bearing mafic magmas, *Contrib. Mineral. Petrol.*, *88*, 217-232, 1984.

Stearns, H.T., and G.A. Macdonald, Geology and ground-water resources of the island of Hawaii, *Hawaii Div. Hydrogr. Bull.*, *9*, 363 pp., 1946.

Stebbins, J.F., I.S.E. Carmichael, and L.K. Moret, Heat capacities and entropies of silicate liquids and glasses, *Contrib. Mineral. Petrol.*, *86*, 131-148, 1984.

Stille, P., D.M. Unruh, and M. Tatsumoto, Pb, Sr, Nd, and Hf isotopic constraints on the origin of Hawaiian basalts and evidence for a unique mantle source, *Geochim. Cosmochim. Acta*, *50*, 2303-2319, 1986.

Stolper, E. and D. Walker, Melt density and the average composition of basalt, *Contrib. Mineral. Petrol.*, *74*, 12, 1980.

Swanson, D.A., Magma supply rate at Kilauea volcano, 1952-1971, *Science*, *175*, 169-170, 1972.

Tatsumoto, M., Isotopic composition of lead in oceanic basalt and its implication to mantle evolution, *Earth Planet. Sci. Lett.*, *38*, 63-87, 1978.

Ten Brink, U.S., and T.M. Brocher, Multichannel seismic evidence for a subcrustal intrusive complex under Oahu and a model for Hawaiian volcanism, *J. Geophys. Res.*, *92*, 13,687-13,707, 1987.

Thompson, R.N., Evidence for a chemical discontinuity near the basalt-andesite transition in many anorogenic volcanic suites, *Nature*, *236*, 106-110, 1972.

Thompson, R.N., Primary basalts and magma genesis, I, Skye, north-west Scotland, *Contrib. Mineral. Petrol.*, *45*, 317-341, 1974.

Tormey, D.R., T.L. Grove, and W.B. Bryan, Experimental petrology of normal MORB near the Kane fracture zone: 22°-25°, Mid-Atlantic Ridge, *Contrib. Mineral. Petrol.*, *96*, 121-139, 1987.

Vaniman, D.T., B.M. Crowe, and E.S. Gladney, Petrology and geochemistry of hawaiite lavas from Crater Flat, Nevada, *Contrib. Mineral. Petrol.*, *80*, 341-357, 1982.

Walker, D., T. Shibata, and S.F. DeLong, Abyssal tholeiites from the Oceanographer Fracture Zone, II; Phase equilibria and mixing, *Contrib. Mineral. Petrol.*, *70*, 111-125, 1979.

West, H.B., and W.P. Leeman, Open system magma chamber processes: Trace element systematics of alkalic cap lavas from Haleakala Crater, Hawaii, paper presented at Hawaii Symposium on How Volcanoes Work, AGU, Hilo, Hawaii, 1987a.

West, H.B., and Leeman, W.P., Isotopic evolution of lavas from Haleakala Crater, Hawaii, *Earth Planet. Sci. Lett.*, *84*, 211-225, 1987b.

West, H.B., M.O. Garcia, F.A. Frey, and A. Kennedy, Nature and cause of compositional variation among the Alkalic Cap Lavas of Mauna Kea Volcano, Hawaii, *Contrib. Mineral. Petrol.*, *100*, 383-397, 1988.

Wilkinson, J.F.G., Undepleted mantle composition beneath Hawaii, *Earth Planet. Sci. Lett.*, *75*, 124-138, 1985.

Wilson, J.T., A possible origin of the Hawaiian islands, *Can. J. Phys.*, *41*, 863-870, 1963.

Wilson, R.E., Mineralogy petrology and geochemistry of basalt weathering, B.S. thesis, LaTrobe Univ., Bundoora, Victoria, Australia, 1978.

Wise, W.S., A volume-time framework for the evolution of Mauna Kea volcano, Hawaii, *Eos Trans. AGU*, *63*, 1137, 1982.

Wright, T.L., Chemistry of Kilauea and Mauna Loa lava in space and time, *U.S. Geol. Surv. Prof. Pap.*, *735*, 40 pp., 1971.

F.A. Frey and A. Kennedy, Department of Earth, Atmospheric, and Planetary Sciences, Room 54-1220, Massachusetts Institute of Technology, Cambridge, MA 02139.

M.O. Garcia and H. West, Hawaii Institute of Geophysics, University of Hawaii, Honolulu, HI 96822.

S.-T. Kwon and W.S. Wise, Department of Geological Sciences, University of California, Santa Barbara, CA 93106.

(Received September 12, 1988;
revised June 22, 1989;
accepted June 26, 1989.)